

# Unsupervised Text Segmentation via Kernel Change-Point Detection on Sentence Embeddings

Mumin Jia <sup>\* 1</sup> Jairo Diaz-Rodriguez <sup>\* 1</sup>

## Abstract

Unsupervised text segmentation is crucial because boundary labels are expensive, subjective, and often fail to transfer across domains and granularity choices. We propose Embed-KCPD, a training-free method that represents sentences as embedding vectors and estimates boundaries by minimizing a penalized KCPD objective. Beyond the algorithmic instantiation, we develop, to our knowledge, the first dependence-aware theory for KCPD under  $m$ -dependent sequences, a finite-memory abstraction of short-range dependence common in language. We prove an oracle inequality for the population penalized risk and a localization guarantee showing that each true change point is recovered within a window that is small relative to segment length. To connect theory to practice, we introduce an LLM-based simulation framework that generates synthetic documents with controlled finite-memory dependence and known boundaries, validating the predicted scaling behavior. Across standard segmentation benchmarks, Embed-KCPD often outperforms strong unsupervised baselines. A case study on Taylor Swift’s tweets illustrates that Embed-KCPD combines strong theoretical guarantees, simulated reliability, and practical effectiveness for text segmentation.

## 1. Introduction

Segmenting a document into coherent topical units is a core subroutine in many NLP and IR systems. Reliable boundaries improve retrieval, summarization, question answering, discourse analysis, and downstream modeling (Prince & Labadié, 2007; Shtekh et al., 2018; Llopis et al., 2002; Cho et al., 2022). Despite this importance, text segmentation is

often a poor fit for standard supervised learning. The “correct” boundary locations depend on the downstream task, the desired granularity, and the annotation protocol, which can vary substantially across corpora. Labels are therefore expensive to obtain, difficult to standardize, and may not transfer cleanly across domains. This makes *unsupervised* segmentation particularly valuable in practice: a method that can be deployed without training labels and remains robust across datasets is often more useful than a narrowly optimized supervised model.

Change-point detection (CPD) provides a natural statistical lens for unsupervised segmentation: boundaries correspond to indices where the data-generating distribution changes. Classical offline CPD methods come with strong guarantees, but these often rest on restrictive assumptions such as Gaussianity, independence, or homoscedasticity (Basseville & Nikiforov, 1993; Bai & Perron, 2003; Killick et al., 2012), which can be brittle for high-dimensional text representations. Kernel change-point detection (KCPD) relaxes much of this structure by comparing distributions through RKHS embeddings, enabling detection of rich distributional shifts without explicit density estimation (Harchaoui & Cappe, 2007; Arlot et al., 2019). This makes KCPD a natural fit for embedding-based segmentation, where modern sentence encoders can reveal semantic changes even when lexical cues are weak. At the same time, deploying KCPD in text exposes a key theoretical limitation: most existing analyses assume independent observations (Garreau & Arlot, 2018), while language exhibits ubiquitous short-range dependence because adjacent units share context, discourse structure, and lexical overlap. This gap motivates dependence-aware guarantees tailored to sequential text.

This paper introduces **Embed-KCPD**, a modular, training-free method for unsupervised text segmentation that combines pretrained sentence embeddings with kernel change-point detection, and provides statistical guarantees for the resulting estimator. Given a sequence of text units  $X_1, \dots, X_T$ , we compute embeddings  $Y_t = f(X_t) \in \mathbb{R}^d$  using a fixed encoder  $f$ . We then estimate change points by minimizing a penalized KCPD objective. KCPD is attractive for this setting because it detects general distributional changes, not only mean shifts, while remaining nonparamet-

<sup>\*</sup>Equal contribution <sup>1</sup>Department of Mathematics and Statistics, York University, Toronto, Canada. Correspondence to: Mumin Jia <amyjia@yorku.ca>, Jairo Diaz-Rodriguez <jdiazrod@yorku.ca>.

ric and compatible with high-dimensional representations (Harchaoui & Cappe, 2007; Arlot et al., 2019). Moreover, the penalized objective can be optimized exactly with dynamic programming and efficiently with pruning (PELT), which makes the method practical for long documents (Killick et al., 2012). The resulting pipeline cleanly decouples representation learning from statistical segmentation, so improvements in sentence encoders can be used immediately without retraining the segmenter.

Beyond proposing a practical method, our goal is to provide a principled foundation for dependent text sequences. To bridge the gap between i.i.d. theory and sequential language, we develop, to our knowledge, the first guarantees for penalized KCPD under  **$m$ -dependence**, a tractable abstraction of finite-memory dependence. While natural language is not literally  $m$ -dependent, this finite-range model offers a clean first approximation to short-range contextual dependence and enables sharp analysis. Under this dependency assumption, we prove an oracle inequality for the population penalized risk and we establish a localization result showing that true change points are recovered within a window whose size is small relative to the segment lengths, yielding vanishing relative error as  $T$  grows.

We connect these results to practice in two complementary ways. First, we introduce a controlled simulation framework that uses an LLM to generate synthetic documents with known change points and explicit finite-memory dependence, enabling stress tests that mirror realistic sequential text while retaining ground truth. Second, we provide a systematic empirical study of Embed-KCPD for text segmentation across standard benchmarks and multiple modern encoders. Across datasets, Embed-KCPD is competitive with established unsupervised baselines and often improves standard segmentation metrics. A case study on a long-running tweet stream illustrates that the discovered segments align with interpretable thematic phases and can support downstream exploratory analysis.

**Contributions.** Our main contributions are: (i) dependence-aware analysis of penalized KCPD under  **$m$ -dependence**, including an oracle inequality and a change-point localization guarantee; (ii) **Embed-KCPD**, a simple, modular, training-free pipeline for **unsupervised** text segmentation that applies offline KCPD to pretrained sentence embeddings; (iii) an LLM-based simulation framework for generating short range dependent text with known boundaries, used to validate the predicted scaling behavior; and (iv) an extensive empirical evaluation on diverse segmentation benchmarks showing that Embed-KCPD is a strong and practical unsupervised baseline.

## 2. Related Work

**Change-point detection methods.** Classical algorithms include Binary Segmentation (Scott & Knott, 1974), dynamic programming (Bai & Perron, 2003), and the Pruned Exact Linear Time (PELT) method (Killick et al., 2012), which offer consistency guarantees under parametric cost functions. Nonparametric approaches relax such assumptions using rank or divergence measures (Aminikhanghahi & Cook, 2017), while kernel methods embed data into reproducing kernel Hilbert spaces (Harchaoui et al., 2008). Recent work explores online and streaming algorithms for real-time detection (Ferrari et al., 2023; Hushchyn et al., 2020), ensemble and statistical inference methods for more reliable boundaries (Duy et al., 2020; Shiraishi et al., 2024), deep kernel learning for adaptive representations (Chang et al., 2019), and unsupervised deep frameworks (Truong et al., 2020).

**Theoretical results on CPD beyond independence.** Beyond independence, CPD under dependence has been studied mainly for parametric or low-dimensional settings: CUSUM/MOSUM with mixing and long-run variance or self-normalization (Csörgő & Horváth, 1997; Aue & Horváth, 2013; Horváth & Rice, 2014), econometric structural-break tests with robust covariances (Andrews, 1993; Bai & Perron, 1998), variance change via ICSS (Inclán & Tiao, 1994), and penalized-contrast methods for dependent series (Lavielle & Moulines, 2000; Lavielle, 2005), with extensions to high-dimensional mean shifts (Cho & Fryzlewicz, 2014; Wang & Samworth, 2017). To our knowledge, we provide the first theoretical results for non-parametric kernel CPD under  $m$ -dependence, aligning theory with modern embedding-based text segmentation.

**Text segmentation methods.** Early methods like TextTiling (Hearst, 1994) exploit lexical cohesion, while later probabilistic approaches, including pLSA-based segmentation (Brants et al., 2002), dynamic programming over TF-IDF similarity (Fragkou et al., 2004), BayesSeg (Eisenstein & Barzilay, 2008), and LDA-based extensions (Riedl & Biemann, 2012; Du et al., 2013), model topical transitions via latent distributions. Recent techniques incorporate coherence-aware segmentation, semantic or embedding signals (Glavaš et al., 2016; Solbiati et al., 2021; Maraj et al., 2024; Yu et al., 2023; Gklezakos et al., 2024); mainly tailored to specific applications, rather than general-purpose text segmentation. In parallel, supervised methods frame segmentation as boundary classification, from attention-based BiLSTMs (Badjatiya et al., 2018) and hierarchical BiLSTMs (Koshorek et al., 2018), to Transformer variants using cross-segment attention (Lukasik et al., 2020) and multi-level Transformer designs (Somasundaran et al., 2020). On the contrary our approach is fully unsupervised text segmentation.

### 3. Preliminaries and Problem

Let  $Y_1, \dots, Y_T \in \mathbb{R}^d$  be an observed sequence. A segmentation of  $1, \dots, T$  into  $K + 1$  contiguous blocks is determined by change points  $\tau_K = (\tau_0, \tau_1, \dots, \tau_K, \tau_{K+1})$  with  $0 = \tau_0 < \tau_1 < \dots < \tau_K < \tau_{K+1} = T$ . We assume there exist true change points  $\tau_K$  such that the distribution of  $(Y_t)$  is piecewise stationary across the  $K + 1$  blocks. The task is to recover both  $K$  and the locations  $\tau_1, \dots, \tau_K$ .

Let  $k : \mathbb{R}^d \times \mathbb{R}^d \rightarrow \mathbb{R}$  be a positive definite kernel with RKHS  $\mathcal{H}$ . The mapping function  $\phi : \mathbb{R}^d \rightarrow \mathcal{H}$  is implicitly defined by  $\phi(y_t) = k(y_t, \cdot) \in \mathcal{H}$ . For distributions  $P, Q$ , the squared maximum mean discrepancy is  $\text{MMD}^2(P, Q) = \|\mu_P - \mu_Q\|_{\mathcal{H}}^2$ . For data  $Y_s, \dots, Y_e$ , define the empirical block cost

$$\widehat{C}(s, e) = \sum_{t=s}^e k(Y_t, Y_t) - \frac{1}{e-s+1} \sum_{i=s}^e \sum_{j=s}^e k(Y_i, Y_j),$$

with expectation  $C(s, e) = \mathbb{E}[\widehat{C}(s, e)]$ . Intuitively,  $\widehat{C}(s, e)$  measures within-block dispersion in RKHS.

**Penalized segmentation criterion.** For a candidate segmentation  $\tau'_{K'}$ , its cost is

$$L(\tau'_{K'}) = \sum_{k=1}^{K'+1} \widehat{C}(\tau'_{k-1} + 1, \tau'_k) + \beta_T K',$$

where  $\beta_T$  penalizes over-segmentation. The kernel change point detection (KCPD) estimator is

$$\widehat{\tau}_{\widehat{K}} = \arg \min_{\tau'_{K'}} L(\tau'_{K'}).$$

$L$  can be minimized exactly with the pruned exact linear time (PELT) algorithm, which under mild conditions has computational cost linear in the document length  $T$ .

### 4. KCPD Under $m$ -Dependence

We now derive our main theoretical results for  $\widehat{\tau}_{\widehat{K}}$  under  $m$ -dependent data. Our goal is to bridge the gap between the classical i.i.d. analyses of kernel change-point detection and the short-range dependence that arises naturally in sequential text, where adjacent units share context, discourse structure, and lexical overlap.

The following assumptions formalize the statistical setting.

**Assumption 4.1** ( $m$ -dependence + within-block stationarity). The sequence  $(Y_t)_{t=1}^T$  is  $m$ -dependent:  $Y_t \perp Y_{t'}$  whenever  $|t - t'| > m$ . Moreover, for each  $k = 1, \dots, K + 1$ , the subsequence  $\{Y_t : \tau_{k-1} < t \leq \tau_k\}$  is strictly stationary with distribution  $P_k$ .

**Assumption 4.2** (kernel). The kernel  $k : \mathbb{R}^d \times \mathbb{R}^d \rightarrow \mathbb{R}$  is bounded and characteristic:  $0 \leq k(x, y) \leq M < \infty$ . Let  $\mathcal{H}$  denote the associated RKHS.

**Assumption 4.3** (detectability). Let  $\mu_{P_k}$  be the RKHS mean embedding of block  $k$  and define  $\Delta_k^2 := \|\mu_{P_k} - \mu_{P_{k+1}}\|_{\mathcal{H}}^2 > 0$ . Set  $\Delta_*^2 := \min_k \Delta_k^2 > 0$ .

**Assumption 4.4** (minimum spacing). The minimal block length satisfies  $\ell_T := \min_k (\tau_k - \tau_{k-1}) \rightarrow \infty$ , and  $\ell_T / \sqrt{T \log T} \rightarrow \infty$  as  $T \rightarrow \infty$ .

**Assumption 4.5** (penalty). The penalty  $\beta_T$  satisfies  $\beta_T \geq 16M\sqrt{2(8m+5)T \log T} + 2M(1+6m)$ ,  $\beta_T = O(\sqrt{T \log T})$ .

**Assumption 4.6** (Admissible Segmentation). The estimator  $\widehat{\tau}_{\widehat{K}}$  is defined as the minimizer of the penalized cost over the set of all partitions where every segment has length at least  $\delta_T$ . We assume  $\delta_T$  satisfies:

$$\delta_T \asymp \sqrt{T \log T} \quad \text{and} \quad \delta_T \leq \ell_T / 3.$$

**Assumption 4.7** (Signal dominance). Let  $\lambda_T = 4\sqrt{2}M\sqrt{(8m+5)\log T}$  and  $\overline{B}_T = (4m+2)M + \frac{(2m^2+2m)M}{\delta_T}$ . There exists  $T_0$  such that for all  $T \geq T_0$ ,

$$\frac{\delta_T}{2} \Delta_*^2 > \beta_T + 3\lambda_T \sqrt{T} + \overline{B}_T.$$

**Assumption 4.8** (Detectability on mixed intervals). There exist constants  $c_0 > 0$ ,  $C_m \geq 0$ , and  $T_0$  such that for all  $T \geq T_0$ , for every pair of consecutive change points  $(\tau_k, \tau_{k+1})$  and interval  $[s, e]$  with  $s \leq \tau_k < \tau_{k+1} \leq e$  and  $e - s + 1 \geq 2\delta_T$ ,

$$\max_{t \in \mathcal{T}_{k,s,e}} \left\{ C(s, e) - C(s, t) - C(t+1, e) \right\} \geq c_0 g_k \Delta_*^2 - C_m, \quad g_k := \tau_{k+1} - \tau_k.$$

where  $\mathcal{T}_{k,s,e} := \{t \in [\tau_k, \tau_{k+1}] : t - s + 1 \geq \delta_T, e - t \geq \delta_T\}$  is the set of admissible split points inside  $[\tau_k, \tau_{k+1}]$  for which both subsegments  $[s, t]$  and  $[t+1, e]$  have length at least  $\delta_T$ .

Assumptions 4.1–4.5 are standard in kernel change-point analysis. Assumption 4.1 allows short-range temporal dependence and assumes stationarity within each block, which is a common regularity condition. Assumption 4.2 (bounded, characteristic kernel) is textbook in MMD/RKHS theory and ensures that the cost is well behaved and that any distributional shift is in principle detectable. Assumption 4.3 is a separation condition that enforces a nontrivial gap between consecutive blocks so that changes are identifiable. Assumption 4.4 guarantees that each block is long enough for reliable estimation, with a mild rate chosen to simplify uniform concentration under dependence. Assumption 4.5 calibrates the penalty at the level of stochastic fluctuations of the empirical cost, preventing severe oversegmentation.

Assumptions 4.6, 4.7 and 4.8 are stronger and are only used for the structural and localization results. Assumption 4.6 excludes very short segments by enforcing a minimum length

at the same order as the concentration rate, which matches the statistical resolution of the problem. Assumption 4.7 requires that, at that scale, the cumulative jump signal dominates both the penalty and random fluctuations. Assumption 4.8 is a detectability condition on mixed intervals that straddle a true change point, ensuring that the best split yields a clear population improvement whenever a genuine change is present. It prevents cancellations so the one-split fit dominates stochastic noise and the penalty, matching the population gain, up to constants. This is reasonable for stationary blocks with a bounded, characteristic kernel.

#### 4.1. Theoretical Results

The first step is to control how well the empirical cost approximates the population cost, uniformly over all segments. A Bernstein type bound for each fixed segment is provided by Proposition A.1 in the appendix. A union bound over all segments yields:

**Lemma 4.9** (uniform deviation over all segments). *Let Assumptions 4.1 and 4.2 hold. Let  $\mathcal{E}_T := \left\{ \forall 1 \leq s \leq e \leq T : |\hat{C}(s, e) - C(s, e)| \leq \lambda_T \sqrt{e - s + 1} \right\}$ . Then, for all integers  $T \geq 3$ ,  $\Pr(\mathcal{E}_T) \geq 1 - T^{-1}$ .*

Informally, the lemma ensures that, with high probability, the empirical cost computed from the data is a good approximation of the corresponding population cost for every segment in the sequence, simultaneously.

As a direct consequence of this concentration and the penalty choice in Assumption 4.5, we obtain a simple structural property on truly homogeneous regions.

**Proposition 4.10** (stability on homogeneous segments). *Let Assumptions 4.1, 4.2, and 4.5 hold. Then, with probability at least  $1 - T^{-1}$ , the following holds simultaneously for every segment  $[s, e]$  that does not contain a true change point (that is,  $\tau_{k-1} < s \leq e < \tau_k$  for some  $k$ ) and every split point  $t$  with  $s \leq t < e$ :*

$$\hat{C}(s, e) < \hat{C}(s, t) + \hat{C}(t+1, e) + \beta_T.$$

In simple terms, in a region where the distribution does not change, inserting an extra change point does not improve the penalized empirical objective, so the procedure has no incentive to create spurious splits inside stationary blocks.

For our first main result, we compare the population performance of the estimated segmentation to that of the best segmentation with the same penalty. This result only requires Assumption 4.1 and 4.2.

**Theorem 4.11** (oracle inequality). *Assume that Assumptions 4.1 and 4.2 hold. With probability at least  $1 - T^{-1}$ ,*

$$\sum_{k=1}^{\hat{K}+1} C(\hat{\tau}_{k-1} + 1, \hat{\tau}_k) + \beta_T \hat{K} \leq$$

$$\inf_{\tau'_{K'}} \left\{ \sum_{k=1}^{K'+1} C(\tau'_{k-1} + 1, \tau'_k) + \beta_T K' \right\} + 2\lambda_T T. \quad (1)$$

This result shows that, in terms of the ideal population criterion, our estimator performs almost as well as the best segmentation that could be chosen with full knowledge of the true block distributions, up to a controlled statistical error term arising from Lemma 4.9.

To understand individual change points, we use the stronger assumptions 4.3–4.8. A key structural consequence, proved via Lemma A.3 and Lemma A.4 in the appendix, is that the estimator does not merge multiple true changes into a single segment. In simple terms, this means that each estimated segment can hide at most one true change point; the procedure does not lump several true changes together into a single segment.

Combined with a strict improvement property for mixed segments (Lemma A.6 in the appendix) and the uniform deviation event  $\mathcal{E}_T$ , this leads to the localization guarantee.

**Theorem 4.12** (localization rate). *Let Assumptions 4.1–4.8 hold. Let  $\delta_T$  be the minimum segment length from Assumption 4.6. Then as  $T \rightarrow \infty$ ,*

$$\Pr\left(\forall 1 \leq k \leq K : \min_{0 \leq j \leq \hat{K}} |\hat{\tau}_j - \tau_k^*| \leq \delta_T\right) \rightarrow 1 \quad (2)$$

In particular,

$$\max_{1 \leq k \leq K} \min_{0 \leq j \leq \hat{K}} |\hat{\tau}_j - \tau_k^*| = O_p(\delta_T).$$

This is a particularly relevant consequence of our analysis: under our signal and spacing assumptions, every true change point is matched by an estimated one within a small window of length  $\delta_T$ , with probability tending to one. The worst case error is therefore of order  $\delta_T$ , and since  $\delta_T$  is much smaller than the minimal block length  $\ell_T$ , this means that the error is tiny compared to the size of each stationary segment, so each change point is recovered at an increasingly precise relative position within its block.

**Remark.** The  $\sqrt{T \log T}$  scaling in  $\delta_T$  is a conservative sufficient condition driven by uniform concentration and a single global penalty. Empirically, our Embed-KCPD performs well on datasets with much shorter segments, and the theory should be interpreted as a conservative sanity guarantee under short-range dependence rather than a practical tuning rule.

#### 5. Embed-KCPD: Instantiation of KCPD for Text Segmentation

We now instantiate Embed-KCPD as a general KCPD framework for text segmentation. The observed sequence

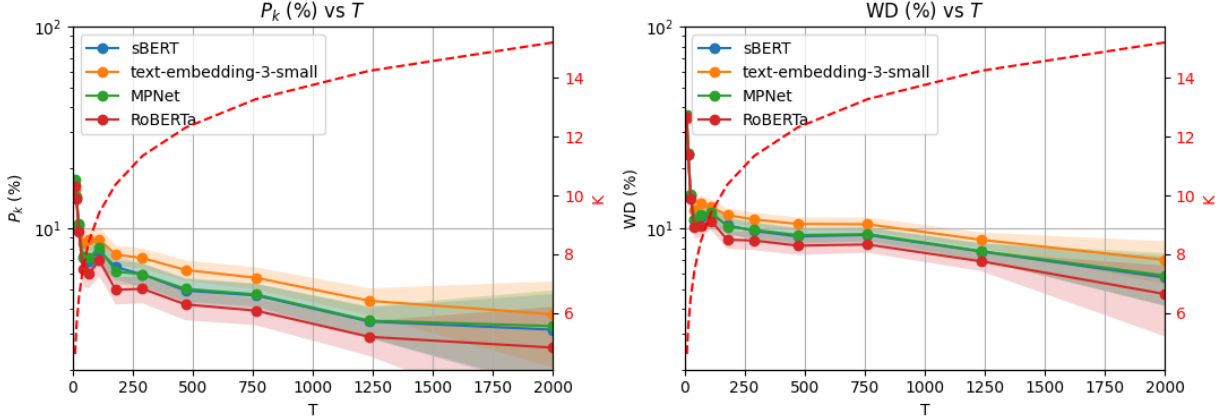


Figure 1. Segmentation accuracies versus sequence length  $T$  for Embed-KCPD applied to synthetically generated short-range dependent text data with GPT-4.1 and  $m = 20$ . Curves compare three embedding methods (sBERT, MPNet, text-embedding-3-small, RoBERTa). Dashed red line shows the growth of the number of change points  $K \approx 2 \log T$ .

$X_1, \dots, X_T$  consists of contiguous text units (sentences, paragraphs, or dialogue turns). Each  $X_t$  is mapped to a normalized vector representation  $Y_t = f(X_t) \in \mathbb{R}^d$ , where  $f$  is a sentence-embedding model.

In the text setting, change points correspond to topic or discourse changes that induce distributional shifts in the embedding space. Assumption 4.1 is natural here: while consecutive sentences are dependent through syntax and discourse, dependence decays quickly, and  $m$ -dependence provides a tractable abstraction of short-range linguistic correlations. Assumption 4.3 requires distinct mean embeddings across segments; this holds whenever topics differ sufficiently in their semantic representation. Assumption 4.4 enforces a minimum segment length, excluding degenerate cases where boundaries occur after only a few sentences; in practice this reflects the fact that coherent topics changes usually span multiple sentences. Finally, Assumption 4.6 corresponds to boundaries being marked by sufficiently salient semantic shifts that cannot be explained by local fluctuations.

We implement two kernels  $k(y, y')$ : a Gaussian RBF, which satisfies Assumption 4.2, and cosine similarity. We include cosine to align with standard NLP practice for sentence embeddings, even though it violates Assumption 4.2 (it is non-characteristic).

**Theory-practice gap.** Our analysis relies on stylized assumptions that act as a tractable proxy for short-range dependence in sequences of sentence embeddings, rather than a literal model of natural language. Consequently, some conditions are worst-case sufficient and likely loose in typical benchmarks. We view the theory as principled support for Embed-KCPD, while the empirical section evaluates performance with pretrained embeddings and efficient kernels (including cosine) under realistic text distributions.

### 5.1. Empirical Evidence of Practical Consistency

To assess the practical reach of theory for Embed-KCPD in text segmentation under controlled conditions with flexible assumptions, we design a simulation with synthetic sequences generated by the large language model GPT-4.1.

We first generate five topic-specific documents (*soccer*, *coffee*, *AI*, *travel*, *dogs*), each with 500 sentences. Within each document, sentences are produced sequentially by prompting GPT4.1 to add one sentence at a time, conditioning on the previous  $m \in \{10, 20, 30\}$  sentences and the document topic; this induces short-range dependence with finite memory and provides clean topic coherence. The resulting process is  $m$ -order Markov rather than strictly  $m$ -dependent, which is often a more realistic abstraction for text, where dependence decays with distance rather than vanishing exactly. Then, for sequence lengths  $T \leq 2000$ , we set the number of change points to  $K = \lceil 2 \log T \rceil$ , randomize change-point locations, and assemble each sequence by concatenating segments drawn from a random selection from the five documents such that consecutive segments have different topics. We generate 100 replicates for each  $(T, K)$ . See details in Appendix D.5. Finally, we estimate change points with Embed-KCPD using four sentence-embedding variants and a penalty of the form  $\beta_T = C \sqrt{T \log T}$ , for  $C \in \{0.001, 0.01, 0.1, 1\}$ , matching the theorem's asymptotic scaling.

**Evaluation metrics.** Following previous work, we evaluate text segmentation with two standard metrics:  $P_k$  (Beeferman et al., 1999) and WindowDiff (WD) (Pevzner & Hearst, 2002).  $P_k$  measures the probability that two sentences within a fixed window are incorrectly assigned to the same or different segments, while WD compares the number of predicted and true boundaries in each window, penalizing both false positives and false negatives. Lower scores indicate better performance. By default, the window size for

Table 1. Performance of Baselines and Embed-KCPD in Choi’s Dataset. The bolded  $P_k$  or WD values denote the best performance for each dataset comparing Embed-KCPD with all baselines.  $x_y$  denotes mean  $x$  with standard deviation  $y$ . \* marks values reported in original papers.

Methods	3-5		6-8		9-11		3-11	
	$P_k \downarrow$	WD $\downarrow$	$P_k \downarrow$	WD $\downarrow$	$P_k \downarrow$	WD $\downarrow$	$P_k \downarrow$	WD $\downarrow$
Unsupervised Methods								
<i>Embed-KCPD (sBERT)</i>								
Cosine kernel	5.2 <sub>5.1</sub>	5.2 <sub>5.1</sub>	3.3 <sub>3.6</sub>	3.4 <sub>3.8</sub>	4.1 <sub>4.6</sub>	4.2 <sub>4.7</sub>	5.7 <sub>5.3</sub>	5.9 <sub>5.4</sub>
RBF kernel	5.4 <sub>5.1</sub>	5.4 <sub>5.1</sub>	6.7 <sub>5.4</sub>	6.7 <sub>5.5</sub>	7.6 <sub>6.6</sub>	7.6 <sub>6.6</sub>	9.2 <sub>7.0</sub>	9.5 <sub>7.1</sub>
<i>Embed-KCPD (MPNet)</i>								
Cosine kernel	4.1 <sub>5.0</sub>	4.1 <sub>5.0</sub>	3.1 <sub>3.6</sub>	3.2 <sub>3.8</sub>	3.8 <sub>4.4</sub>	3.8 <sub>4.4</sub>	5.7 <sub>5.5</sub>	5.9 <sub>5.7</sub>
RBF kernel	4.4 <sub>5.1</sub>	4.4 <sub>5.1</sub>	5.1 <sub>5.2</sub>	5.1 <sub>5.2</sub>	6.3 <sub>6.6</sub>	6.3 <sub>6.6</sub>	7.7 <sub>6.1</sub>	8.0 <sub>6.3</sub>
<i>Embed-KCPD (text-embedding-3-small)</i>								
Cosine kernel	<b>3.6</b> <sub>4.3</sub>	<b>3.6</b> <sub>4.3</sub>	<b>2.5</b> <sub>3.3</sub>	<b>2.6</b> <sub>3.4</sub>	3.1 <sub>4.7</sub>	3.1 <sub>4.7</sub>	5.2 <sub>5.4</sub>	5.4 <sub>5.5</sub>
RBF kernel	3.9 <sub>4.4</sub>	3.9 <sub>4.4</sub>	4.6 <sub>5.3</sub>	4.7 <sub>5.4</sub>	5.6 <sub>5.2</sub>	7.3 <sub>6.4</sub>	7.6 <sub>6.5</sub>	5.3 <sub>5.3</sub>
<i>Embed-KCPD (RoBERTa)</i>								
Cosine kernel	4.1 <sub>4.8</sub>	4.1 <sub>4.8</sub>	2.9 <sub>3.5</sub>	3.1 <sub>3.8</sub>	3.4 <sub>4.3</sub>	3.6 <sub>4.4</sub>	5.0 <sub>5.2</sub>	5.3 <sub>5.4</sub>
RBF kernel	4.3 <sub>5.0</sub>	4.3 <sub>5.0</sub>	4.9 <sub>5.0</sub>	5.0 <sub>5.0</sub>	5.7 <sub>5.5</sub>	5.7 <sub>5.5</sub>	8.0 <sub>6.2</sub>	8.3 <sub>6.3</sub>
<i>Baselines</i>								
Coherence	4.4*	6.2*	3.1*	3.3*	<b>2.5</b> *	<b>2.6</b> *	<b>4.0</b> *	<b>4.4</b> *
GraphSeg	5.6*	8.7*	7.2*	9.4*	6.6*	9.6*	7.2*	9.0*
TextTiling	44*	—	43*	—	48*	—	46*	—
TextTiling (MPNet)	44.6 <sub>5.6</sub>	86.3 <sub>9.6</sub>	37.6 <sub>6.4</sub>	76.7 <sub>10.1</sub>	31.1 <sub>5.4</sub>	70.1 <sub>8.8</sub>	31.7 <sub>6.6</sub>	71.5 <sub>9.6</sub>
TextTiling (sBERT)	50.0 <sub>3.5</sub>	96.9 <sub>3.6</sub>	45.3 <sub>5.1</sub>	91.7 <sub>4.6</sub>	40.3 <sub>4.3</sub>	86.6 <sub>5.4</sub>	41.2 <sub>5.9</sub>	86.8 <sub>6.6</sub>
Choi (Choi, 2000)	12.0*	—	9.0*	—	9.0*	—	12.0*	—
Brants et al. (2002)	7.4*	—	8.0*	—	6.8*	—	19.7*	—
Fragkou et al. (2004)	5.5*	—	3.0*	—	1.3*	—	7.0*	—
Misra et al. (2009)	23.0*	—	15.8*	—	14.4*	—	16.1*	—

both metrics is set to half the average true segment length. We adopt the same metrics for the experiments in Sec. 6.

**Results.** Figures 3 and 4 in Appendix C summarize results on  $P_k$  varying  $C$  and  $m$ . The value  $C = 0.1$  yields the best stable asymptotic performance as  $T$  increases, consistent with our theoretical scaling. Although this value is smaller than the conservative lower bound in our assumptions, such under-penalization is common in practice: it increases sensitivity to boundaries while preserving the prescribed asymptotic rate. Results also indicate that the asymptotics are not sensitive to the value of  $m$ , which is in practice unknown. Full results for  $C = 0.1$  and  $m = 20$  are shown in Fig. 1. Empirically,  $P_k$  and WD decrease as  $T$  grows (with  $K$  scaling as above), indicating improved segmentation accuracy consistent with our asymptotic guarantees on change-point recovery; despite the theoretical assumptions being only partially satisfied.

## 6. Experimental Evaluation

**Datasets.** We evaluate our methods on several widely used datasets for text segmentation. Choi’s dataset (Choi, 2000), consisting of 700 synthetic documents, serves as the bench-

mark for segmentation performance. Wiki-300, introduced by (Badjatiya et al., 2018), contains 300 documents. We also include two smaller datasets: Wiki-50 introduced by Koshorek et al. (2018) and Elements (Chen et al., 2009) about 118 chemical elements. In addition, we construct a new dataset of 20 documents by randomly selecting some recent abstracts from arXiv paper and concatenating them to form one document, to add a clean dataset unknown to all baseline methods. A summary of dataset statistics is presented in Table D.1. The detailed procedure for constructing the arXiv dataset is in Appendix D.6.

**Experimental details.** For each dataset, we apply Embed-KCPD with both the cosine and RBF kernels, using four modern sentence embeddings for text segmentation: sBERT (Reimers & Gurevych, 2019), MPNet (Song et al., 2020), text-embedding-3-small (OpenAI, 2025), and RoBERTa (Liu et al., 2019). As unsupervised baselines, we include TextTiling (Hearst, 1994), GraphSeg (Glavaš et al., 2016), and Coherence (Maraj et al., 2024), and compare their performance with Embed-KCPD across all datasets. We also compare with a modern version of TextTiling using modern embeddings, following saeedabc (2025) tuning configuration for sBERT and MPNet embeddings. For the comparison

Table 2. Performance of Baselines and Embed-KCPD in Wikipedia, Elements and arXiv Dataset. The bolded  $P_k$  or WD values denote values where Embed-KCPD surpassed all unsupervised baselines. The last 3 rows serve only as a reference on supervised methods.  $x_y$  denotes mean  $x$  with standard deviation  $y$ . \* indicates values reported from the original papers.

Methods	Wiki-300		Wiki-50		Elements		arXiv	
	$P_k \downarrow$	WD $\downarrow$	$P_k \downarrow$	WD $\downarrow$	$P_k \downarrow$	WD $\downarrow$	$P_k \downarrow$	WD $\downarrow$
Unsupervised Methods								
<i>Embed-KCPD (sBERT)</i>								
Cosine kernel	<b>33.9</b> <sub>13.0</sub>	<b>35.2</b> <sub>12.3</sub>	42.4 <sub>15.1</sub>	<b>43.8</b> <sub>15.3</sub>	<b>40.0</b> <sub>15.9</sub>	47.5 <sub>15.9</sub>	<b>7.9</b> <sub>7.2</sub>	<b>8.2</b> <sub>7.6</sub>
RBF kernel	<b>34.2</b> <sub>12.6</sub>	<b>37.3</b> <sub>13.7</sub>	47.2 <sub>17.4</sub>	51.9 <sub>21.0</sub>	<b>33.3</b> <sub>15.9</sub>	44.0 <sub>16.6</sub>	<b>11.2</b> <sub>9.5</sub>	<b>11.8</b> <sub>10.1</sub>
<i>Embed-KCPD (MPNet)</i>								
Cosine kernel	<b>33.2</b> <sub>12.6</sub>	<b>34.4</b> <sub>11.7</sub>	40.5 <sub>16.2</sub>	<b>42.0</b> <sub>16.8</sub>	<b>41.1</b> <sub>16.4</sub>	47.6 <sub>16.0</sub>	<b>9.1</b> <sub>9.1</sub>	<b>9.2</b> <sub>9.1</sub>
RBF kernel	<b>34.0</b> <sub>11.9</sub>	<b>35.1</b> <sub>11.3</sub>	44.8 <sub>17.3</sub>	49.3 <sub>20.1</sub>	<b>32.9</b> <sub>16.2</sub>	43.3 <sub>16.2</sub>	<b>14.7</b> <sub>11.1</sub>	<b>15.7</b> <sub>12.0</sub>
<i>Embed-KCPD (text-embedding-3-small)</i>								
Cosine kernel	<b>32.8</b> <sub>12.8</sub>	<b>33.8</b> <sub>12.0</sub>	<b>38.0</b> <sub>14.7</sub>	<b>39.8</b> <sub>15.8</sub>	44.9 <sub>17.4</sub>	50.3 <sub>16.7</sub>	<b>9.2</b> <sub>9.8</sub>	<b>9.3</b> <sub>9.9</sub>
RBF kernel	<b>33.8</b> <sub>12.6</sub>	<b>34.7</b> <sub>12.0</sub>	43.9 <sub>17.0</sub>	48.5 <sub>20.5</sub>	<b>32.1</b> <sub>16.3</sub>	43.0 <sub>17.4</sub>	<b>11.3</b> <sub>10.6</sub>	<b>11.7</b> <sub>11.0</sub>
<i>Embed-KCPD (RoBERTa)</i>								
Cosine kernel	<b>32.4</b> <sub>12.8</sub>	<b>33.7</b> <sub>11.9</sub>	39.5 <sub>14.7</sub>	<b>41.6</b> <sub>15.5</sub>	<b>37.8</b> <sub>18.7</sub>	45.5 <sub>17.9</sub>	<b>8.3</b> <sub>7.9</sub>	<b>8.8</b> <sub>8.6</sub>
RBF kernel	<b>33.1</b> <sub>12.9</sub>	<b>34.3</b> <sub>12.1</sub>	44.5 <sub>17.2</sub>	49.2 <sub>20.4</sub>	<b>33.8</b> <sub>16.5</sub>	45.4 <sub>16.8</sub>	<b>10.7</b> <sub>9.4</sub>	<b>11.7</b> <sub>10.1</sub>
<i>Baselines</i>								
Coherence	50.2*	53.4*	53.5 <sub>12.3</sub>	71.1 <sub>18.4</sub>	42.4 <sub>18.1</sub>	54.7 <sub>16.6</sub>	43.0 <sub>8.9</sub>	45.4 <sub>9.3</sub>
GraphSeg	50.7 <sub>11.4</sub>	54.8 <sub>12.8</sub>	50.2 <sub>17.1</sub>	50.9 <sub>18.7</sub>	52.9 <sub>19.3</sub>	42.3 <sub>16.3</sub>	29.0 <sub>11.7</sub>	29.1 <sub>12.1</sub>
TextTiling	60.3 <sub>9.1</sub>	66.3 <sub>11.2</sub>	47.6 <sub>11.8</sub>	48.3 <sub>11.8</sub>	49.6 <sub>18.3</sub>	50.4 <sub>20.5</sub>	47.9 <sub>9.1</sub>	40.1 <sub>7.7</sub>
TextTiling (MPNet)	38.1 <sub>12.4</sub>	46.0 <sub>14.3</sub>	38.9 <sub>14.5</sub>	44.6 <sub>15.4</sub>	60.8 <sub>19.3</sub>	60.8 <sub>19.3</sub>	27.1 <sub>7.2</sub>	39.9 <sub>7.9</sub>
TextTiling (sBERT)	41.1 <sub>14.6</sub>	53.8 <sub>18.9</sub>	40.7 <sub>13.8</sub>	49.8 <sub>19.0</sub>	60.8 <sub>19.0</sub>	60.9 <sub>18.9</sub>	34.8 <sub>8.3</sub>	73.7 <sub>10.5</sub>
Supervised Methods								
<i>NTS</i>	<b>34.4</b> *	<b>31.5</b> *	—	—	—	—	—	—
<i>CATS</i>	—	—	<b>16.5</b> *	—	<b>18.4</b> *	—	—	—
<i>TextSeg</i>	—	—	<b>18.2</b> *	—	<b>41.6</b> *	—	—	—

of Choi’s dataset (Choi, 2000), we further compare other unsupervised methods, (Choi, 2000; Brants et al., 2002; Frakou et al., 2004; Misra et al., 2009). See Appendix D.2 for more implementation details. For the Wikipedia-based datasets, we additionally include supervised approaches reported in prior work: NTS (Badjatiya et al., 2018), CATS (Somasundaran et al., 2020), TextSeg (Koshorek et al., 2018). We use  $\beta_T = C \sqrt{T} \log T$ .

We select a single global  $C$  using an unsupervised elbow method, setting  $C = 0.06$  for the RBF kernel and  $C = 0.088$  for the cosine kernel across all benchmarks (see Appendix D.3 for details). Figure 11 in Appendix indicates that performance remains stable across a range of  $C$  values.

## 6.1. Main Results

### 6.1.1. RESULTS ON CHOI’S DATASET

Table 1 reports performance on the synthetic Choi benchmark. Across all settings, Embed-KCPD with a cosine kernel consistently outperforms the RBF kernel, especially for group 3-11, despite the cosine kernel falls outside our theoretical guarantees. This behavior reflects the highly stylized

nature of Choi’s dataset: documents are extremely short and segment boundaries are dominated by sharp topic shifts in lexical overlap. In such settings, cosine similarity appears better suited to capturing these discontinuities. Among embeddings, text-embedding-3-small combined with cosine kernel achieves the strongest overall performance. More generally, Embed-KCPD exhibits stable and consistent performance across kernels and embeddings. While Coherence achieves the best scores on the 3-11 and 9-11 groups, Embed-KCPD delivers competitive results on a dataset that is widely used in the literature, despite being highly artificial relative to real-world text segmentation tasks.

### 6.1.2. RESULTS ON OTHER BENCHMARKS

Table 2 summarizes results on more realistic datasets: Wiki-300, Wiki-50, Elements, and arXiv. We include supervised methods for reference.

**Comparing Embed-KCPD to unsupervised baselines.** Embed-KCPD variants outperform all baselines across most datasets and evaluation metrics. As shown in Table 2, Embed-KCPD achieves lower  $P_k$  and WD in nearly all settings, with few exceptions. Importantly, even when Text-

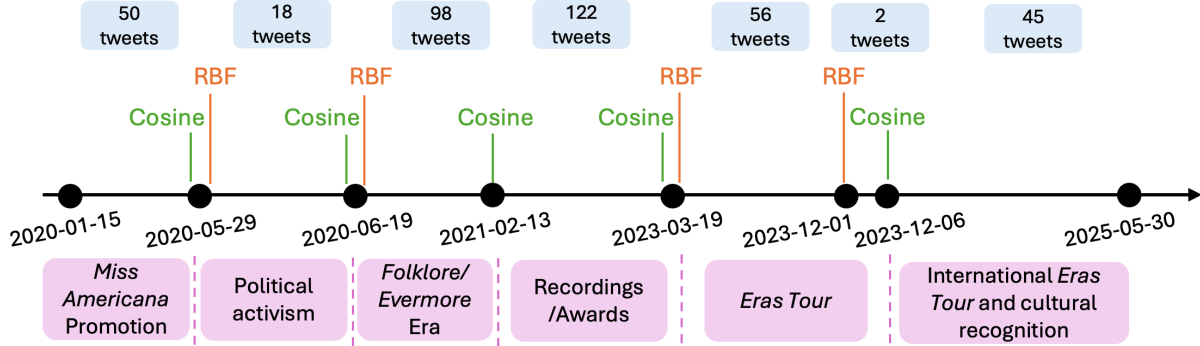


Figure 2. Timeline of Taylor Swift’s tweet stream segmented by Embed-KCPD using RBF and cosine kernels. Each segment is annotated with its tweet count (blue boxes) and an interpretation of its content (pink boxes).

Tiling is augmented with sentence embeddings, Embed-KCPD typically achieves superior performance, indicating that its gains are not solely attributable to the use of embeddings. These results demonstrate the effectiveness of Embed-KCPD as an unsupervised method.

**Comparing kernels and embeddings.** Results with Embed-KCPD using RBF and cosine kernels are more balanced than in Choi’s dataset: the cosine kernel surpasses the RBF on Wiki-300, Wiki-50, and arXiv datasets, while RBF achieves stronger performance on Elements. This variation suggests that our theoretical framework, though developed for characteristic kernels, does not preclude competitive results with alternatives in practice. Among embeddings, text-embedding-3-small yields the lowest  $P_k$  and WD on Wiki-50, while RoBERTa achieves the lowest score on the remaining three datasets. Overall, performance differences across embeddings are modest, underscoring the robustness of Embed-KCPD to both kernel and embedding choices.

**Comparing Embed-KCPD with supervised methods.** On Wiki-300, Embed-KCPD achieves lower  $P_k$  than [Badjatiya et al. \(2018\)](#) across all embeddings and kernels, with WD approaching the supervised baseline. On Elements, Embed-KCPD attains lower  $P_k$  than [Koshorek et al. \(2018\)](#) for most kernel-embedding combinations, with the exception of the kCPD kernel paired with text-embedding-3-small, where performance remains close. These findings suggest that Embed-KCPD, despite being unsupervised, achieves performance comparable to strong supervised methods.

## 7. Case Study

To demonstrate Embed-KCPD’s practical value, we include a real-world case study on social-media data: 391 Taylor Swift tweets collected from January 2020 through May 2025. This example shows how a practitioner can readily apply Embed-KCPD to detect topical shifts and conduct downstream analysis in a realistic setting.

**Experimental details.** Consistent with Sec. 6.1, we use

text-embedding-3-small, which delivers strong segmentation across benchmarks. Following the same procedure used for the benchmark datasets, we choose  $C$  via the elbow method (Fig. 10 in Appendix), yielding  $C = 0.03$  for Embed-KCPD with an RBF kernel and  $C = 0.04$  for the cosine kernel. Using these settings, we apply Embed-KCPD to Taylor Swift’s tweet stream with both kernels and analyze the resulting segments. The detected breakpoints appear on the timeline in Fig. 2.

**Interpretation.** The first segment aligns with *Miss Americana* promotion and early COVID-19 reflections (Jan–May 2020). The second reflects heightened political engagement (May–Jun 2020). A third segment, captured only by the cosine kernel, covers the *folklore/evermore* era (Jun 2020–Feb 2021), followed by an extended recording/awards period (Feb 2021–Mar 2023). The first year of the famous *Eras Tour* marks the next segment (Mar–Dec 2023). We observe a minor discrepancy between RBF and cosine in the end date of this segment, which we treat as the same change point in practice. The final segment (Dec 2023–May 2025) corresponds to re-releases and broader cultural recognition. Overall, the detected boundaries closely track well-known events in Taylor Swift’s timeline, illustrating Embed-KCPD’s ability to recover meaningful shifts in text streams.

## 8. Conclusion

We performed both a theoretical and empirical study of kernel change-point detection under  $m$ -dependence by proving an oracle inequality and consistency in change points locations. Building on this, we instantiated Embed-KCPD for unsupervised text segmentation and presented a comprehensive empirical evaluation, demonstrating strong performance against baselines and applicability in a real dataset. In doing so, we bridge theoretical guarantees with practical effectiveness, highlighting Embed-KCPD as an applicable framework for text segmentation.

## Impact Statement

This paper presents work whose goal is to advance the field of Machine Learning. There are many potential societal consequences of our work, none which we feel must be specifically highlighted here.

## References

Aminikhanghahi, S. and Cook, D. J. A survey of methods for time series change point detection. *Knowledge and Information Systems*, 51(2):339–367, 2017. ISSN 0219-3116. doi: 10.1007/s10115-016-0987-z. URL <https://doi.org/10.1007/s10115-016-0987-z>.

Andrews, D. W. K. Tests for parameter instability and structural change with unknown change point. *Econometrica*, 61(4):821–856, 1993. ISSN 00129682, 14680262. URL <http://www.jstor.org/stable/2951764>.

Arlot, S., Celisse, A., and Harchaoui, Z. A kernel multiple change-point algorithm via model selection. *Journal of Machine Learning Research*, 20(162):1–56, 2019. URL <http://jmlr.org/papers/v20/16-155.html>.

Aue, A. and Horváth, L. Structural breaks in time series. *Journal of Time Series Analysis*, 34(1):1–16, 2013. doi: <https://doi.org/10.1111/j.1467-9892.2012.00819.x>. URL <https://onlinelibrary.wiley.com/doi/abs/10.1111/j.1467-9892.2012.00819.x>.

Badjatiya, P., Kurisinkel, L. J., Gupta, M., and Varma, V. Attention-based neural text segmentation. In Pasi, G., Piwowarski, B., Azzopardi, L., and Hanbury, A. (eds.), *Advances in Information Retrieval*, pp. 180–193, Cham, 2018. Springer International Publishing. ISBN 978-3-319-76941-7.

Bai, J. and Perron, P. Estimating and testing linear models with multiple structural changes. *Econometrica*, 66(1): 47–78, 1998. ISSN 00129682, 14680262. URL <http://www.jstor.org/stable/2998540>.

Bai, J. and Perron, P. Computation and analysis of multiple structural change models. *Journal of Applied Econometrics*, 18(1):1–22, 2003. doi: <https://doi.org/10.1002/jae.659>. URL <https://onlinelibrary.wiley.com/doi/abs/10.1002/jae.659>.

Basseville, M. and Nikiforov, I. *Detection of Abrupt Change Theory and Application*, volume 15. 04 1993. ISBN 0-13-126780-9.

Beeferman, D., Berger, A., and Lafferty, J. Statistical models for text segmentation. *Machine Learning*, 34 (1):177–210, 1999. ISSN 1573-0565. doi: 10.1023/A:1007506220214. URL <https://doi.org/10.1023/A:1007506220214>.

Brants, T., Chen, F., and Tschantzidis, I. Topic-based document segmentation with probabilistic latent semantic analysis. In *Proceedings of the Eleventh International Conference on Information and Knowledge Management*, CIKM ’02, pp. 211–218, New York, NY, USA, 2002. Association for Computing Machinery. ISBN 1581134924. doi: 10.1145/584792.584829. URL <https://doi.org/10.1145/584792.584829>.

Chang, W.-C., Li, C.-L., Yang, Y., and Póczos, B. Kernel change-point detection with auxiliary deep generative models. In *International Conference on Learning Representations*, 2019. URL <https://openreview.net/forum?id=r1GbfhRqF7>.

Chen, H., Branavan, S., Barzilay, R., and Karger, D. R. Global models of document structure using latent permutations. In Ostendorf, M., Collins, M., Narayanan, S., Oard, D. W., and Vanderwende, L. (eds.), *Proceedings of Human Language Technologies: The 2009 Annual Conference of the North American Chapter of the Association for Computational Linguistics*, pp. 371–379, Boulder, Colorado, June 2009. Association for Computational Linguistics. URL <https://aclanthology.org/N09-1042/>.

Cho, H. and Fryzlewicz, P. Multiple-change-point detection for high dimensional time series via sparsified binary segmentation. *Journal of the Royal Statistical Society Series B: Statistical Methodology*, 77(2):475–507, 07 2014. ISSN 1369-7412. doi: 10.1111/rssb.12079. URL <https://doi.org/10.1111/rssb.12079>.

Cho, S., Song, K., Wang, X., Liu, F., and Yu, D. Toward unifying text segmentation and long document summarization. In Goldberg, Y., Kozareva, Z., and Zhang, Y. (eds.), *Proceedings of the 2022 Conference on Empirical Methods in Natural Language Processing*, pp. 106–118, Abu Dhabi, United Arab Emirates, December 2022. Association for Computational Linguistics. doi: 10.18653/v1/2022.emnlp-main.8. URL [https://aclanthology.org/2022.emnlp-main.8/](https://aclanthology.org/2022.emnlp-main.8).

Choi, F. Y. Y. Advances in domain independent linear text segmentation. In *1st Meeting of the North American Chapter of the Association for Computational Linguistics*, 2000. URL <https://aclanthology.org/A00-2004/>.

Csörgö, M. and Horváth, L. *Limit Theorems in Change-Point Analysis*. Wiley Series in Probability and Statistics. Wiley, 1997. ISBN 9780471955221. URL <https://books.google.ca/books?id=iyXvAAAAMAAJ>.

Du, L., Buntine, W., and Johnson, M. Topic segmentation with a structured topic model. In Vanderwende, L., Daumé III, H., and Kirchhoff, K. (eds.), *Proceedings of the 2013 Conference of the North American Chapter of the Association for Computational Linguistics: Human Language Technologies*, pp. 190–200, Atlanta, Georgia, June 2013. Association for Computational Linguistics. URL <https://aclanthology.org/N13-1019/>.

Duy, V. N. L., Toda, H., Sugiyama, R., and Takeuchi, I. Computing valid p-value for optimal changepoint by selective inference using dynamic programming. In Larochelle, H., Ranzato, M., Hadsell, R., Balcan, M., and Lin, H. (eds.), *Advances in Neural Information Processing Systems*, volume 33, pp. 11356–11367. Curran Associates, Inc., 2020. URL [https://proceedings.neurips.cc/paper\\_files/paper/2020/file/82b04cd5aa016d979fe048f3ddf0e8d3-Paper.pdf](https://proceedings.neurips.cc/paper_files/paper/2020/file/82b04cd5aa016d979fe048f3ddf0e8d3-Paper.pdf).

Eisenstein, J. and Barzilay, R. Bayesian unsupervised topic segmentation. In Lapata, M. and Ng, H. T. (eds.), *Proceedings of the 2008 Conference on Empirical Methods in Natural Language Processing*, pp. 334–343, Honolulu, Hawaii, October 2008. Association for Computational Linguistics. URL <https://aclanthology.org/D08-1035/>.

Ferrari, A., Richard, C., Bourrier, A., and Bouchikhi, I. Online change-point detection with kernels. *Pattern Recognition*, 133:109022, 2023. ISSN 0031-3203. doi: <https://doi.org/10.1016/j.patcog.2022.109022>. URL <https://www.sciencedirect.com/science/article/pii/S0031320322005027>.

Fragkou, P., Petridis, V., and Kehagias, A. A dynamic programming algorithm for linear text segmentation. *Journal of Intelligent Information Systems*, 23(2):179–197, 2004. doi: [10.1023/B:JIIS.0000039534.65423.00](https://doi.org/10.1023/B:JIIS.0000039534.65423.00). URL <https://doi.org/10.1023/B:JIIS.0000039534.65423.00>.

Garreau, D. and Arlot, S. Consistent change-point detection with kernels. *Electronic Journal of Statistics*, 12(2):4440–4486, 2018. doi: [10.1214/18-EJS1513](https://doi.org/10.1214/18-EJS1513). URL <https://doi.org/10.1214/18-EJS1513>.

Gklezakos, D. C., Misiak, T., and Bishop, D. Treeseg: Hierarchical topic segmentation of large transcripts, 2024. URL <https://arxiv.org/abs/2407.12028>.

Glavaš, G., Nanni, F., and Ponzetto, S. P. Unsupervised text segmentation using semantic relatedness graphs. In Gardent, C., Bernardi, R., and Titov, I. (eds.), *Proceedings of the Fifth Joint Conference on Lexical and Computational Semantics*, pp. 125–130, Berlin, Germany, August 2016. Association for Computational Linguistics. doi: [10.18653/v1/S16-2016](https://doi.org/10.18653/v1/S16-2016). URL <https://aclanthology.org/S16-2016/>.

Harchaoui, Z. and Cappe, O. Retrospective multiple changepoint estimation with kernels. In *2007 IEEE/SP 14th Workshop on Statistical Signal Processing*, pp. 768–772, 2007. doi: [10.1109/SSP.2007.4301363](https://doi.org/10.1109/SSP.2007.4301363).

Harchaoui, Z., Moulines, E., and Bach, F. Kernel change-point analysis. In Koller, D., Schuurmans, D., Bengio, Y., and Bottou, L. (eds.), *Advances in Neural Information Processing Systems*, volume 21. Curran Associates, Inc., 2008. URL [https://proceedings.neurips.cc/paper\\_files/paper/2008/file/08b255a5d42b89b0585260b6f2360bdd-Paper.pdf](https://proceedings.neurips.cc/paper_files/paper/2008/file/08b255a5d42b89b0585260b6f2360bdd-Paper.pdf).

Hearst, M. A. Multi-paragraph segmentation expository text. In *32nd Annual Meeting of the Association for Computational Linguistics*, pp. 9–16, Las Cruces, New Mexico, USA, June 1994. Association for Computational Linguistics. doi: [10.3115/981732.981734](https://doi.org/10.3115/981732.981734). URL <https://aclanthology.org/P94-1002/>.

Horváth, L. and Rice, G. Extensions of some classical methods in change point analysis. *TEST*, 23(2):219–255, 2014. doi: [10.1007/s11749-014-0368-4](https://doi.org/10.1007/s11749-014-0368-4).

Hushchyn, M., Arzamatov, K., and Derkach, D. Online neural networks for change-point detection, 2020. URL <https://arxiv.org/abs/2010.01388>.

Inclán, C. and Tiao, G. C. Use of cumulative sums of squares for retrospective detection of changes of variance. *Journal of the American Statistical Association*, 89(427):913–923, 1994. ISSN 01621459, 1537274X. URL [http://www.jstor.org/stable/2290916](https://www.jstor.org/stable/2290916).

Janson, S. Large deviations for sums of partly dependent random variables. *Random Structures & Algorithms*, 24(3):234–248, 2004. doi: <https://doi.org/10.1002/rsa.20008>. URL <https://onlinelibrary.wiley.com/doi/abs/10.1002/rsa.20008>.

Killick, R., Fearnhead, P., and Eckley, I. A. Optimal detection of changepoints with a linear computational cost. *Journal of the American Statistical Association*, 107(500):1590–1598, 2012. doi: [10.1080/01621459.2012.737745](https://doi.org/10.1080/01621459.2012.737745). URL <https://doi.org/10.1080/01621459.2012.737745>.

Koshorek, O., Cohen, A., Mor, N., Rotman, M., and Berant, J. Text segmentation as a supervised learning task. In Walker, M., Ji, H., and Stent, A. (eds.), *Proceedings of the 2018 Conference of the North American Chapter of*

the Association for Computational Linguistics: Human Language Technologies, Volume 2 (Short Papers), pp. 469–473, New Orleans, Louisiana, June 2018. Association for Computational Linguistics. doi: 10.18653/v1/N18-2075. URL <https://aclanthology.org/N18-2075/>.

Lavielle, M. Using penalized contrasts for the change-point problem. *Signal Processing*, 85(8):1501–1510, 2005. ISSN 0165-1684. doi: <https://doi.org/10.1016/j.sigpro.2005.01.012>. URL <https://www.sciencedirect.com/science/article/pii/S0165168405000381>.

Lavielle, M. and Moulines, E. Least-squares estimation of an unknown number of shifts in a time series. *Journal of Time Series Analysis*, 21(1):33–59, 2000. doi: <https://doi.org/10.1111/1467-9892.00172>. URL <https://onlinelibrary.wiley.com/doi/abs/10.1111/1467-9892.00172>.

Liu, Y., Ott, M., Goyal, N., Du, J., Joshi, M., Chen, D., Levy, O., Lewis, M., Zettlemoyer, L., and Stoyanov, V. Roberta: A robustly optimized bert pretraining approach, 2019. URL <https://arxiv.org/abs/1907.11692>.

Llopis, F., Rodríguez, A. F., and González, J. L. V. Text segmentation for efficient information retrieval. In *Proceedings of the Third International Conference on Computational Linguistics and Intelligent Text Processing, CICLing '02*, pp. 373–380, Berlin, Heidelberg, 2002. Springer-Verlag. ISBN 3540432191.

Lukasik, M., Dadachev, B., Papineni, K., and Simões, G. Text segmentation by cross segment attention. In Webber, B., Cohn, T., He, Y., and Liu, Y. (eds.), *Proceedings of the 2020 Conference on Empirical Methods in Natural Language Processing (EMNLP)*, pp. 4707–4716, Online, November 2020. Association for Computational Linguistics. doi: 10.18653/v1/2020.emnlp-main.380. URL [https://aclanthology.org/2020.emnlp-main.380/](https://aclanthology.org/2020.emnlp-main.380).

Maraj, A., Vargas Martin, M., and Makrehchi, M. Words that stick: Using keyword cohesion to improve text segmentation. In Barak, L. and Alikhani, M. (eds.), *Proceedings of the 28th Conference on Computational Natural Language Learning*, pp. 1–9, Miami, FL, USA, November 2024. Association for Computational Linguistics. doi: 10.18653/v1/2024.conll-1.1. URL <https://aclanthology.org/2024.conll-1.1/>.

Misra, H., Yvon, F., Jose, J. M., and Cappe, O. Text segmentation via topic modeling: an analytical study. In *Proceedings of the 18th ACM Conference on Information and Knowledge Management, CIKM '09*, pp. 1553–1556, New York, NY, USA, 2009. Association for Computing Machinery. ISBN 9781605585123. doi: 10.1145/1645953.1646170. URL <https://doi.org/10.1145/1645953.1646170>.

OpenAI. *OpenAI Platform Documentation*, 2025. URL <https://platform.openai.com/docs/overview>.

Pevzner, L. and Hearst, M. A. A critique and improvement of an evaluation metric for text segmentation. *Computational Linguistics*, 28(1):19–36, 2002. doi: 10.1162/089120102317341756. URL <https://aclanthology.org/J02-1002/>.

Prince, V. and Labadié, A. Text segmentation based on document understanding for information retrieval. In Kedad, Z., Lammar, N., Métais, E., Meziane, F., and Rezgui, Y. (eds.), *Natural Language Processing and Information Systems*, pp. 295–304, Berlin, Heidelberg, 2007. Springer Berlin Heidelberg. ISBN 978-3-540-73351-5.

Reimers, N. and Gurevych, I. Sentence-BERT: Sentence embeddings using Siamese BERT-networks. In Inui, K., Jiang, J., Ng, V., and Wan, X. (eds.), *Proceedings of the 2019 Conference on Empirical Methods in Natural Language Processing and the 9th International Joint Conference on Natural Language Processing (EMNLP-IJCNLP)*, pp. 3982–3992, Hong Kong, China, November 2019. Association for Computational Linguistics. doi: 10.18653/v1/D19-1410. URL <https://aclanthology.org/D19-1410/>.

Riedl, M. and Biemann, C. TopicTiling: A text segmentation algorithm based on LDA. In Cheung, J. C. K., Hatori, J., Henriquez, C., and Irvine, A. (eds.), *Proceedings of ACL 2012 Student Research Workshop*, pp. 37–42, Jeju Island, Korea, July 2012. Association for Computational Linguistics. URL <https://aclanthology.org/W12-3307/>.

saeedabc. Extended texttiling using llm embeddings for text segmentation. <https://github.com/saeedabc/llm-text-tiling>, 2025. [Software].

Scott, A. J. and Knott, M. A cluster analysis method for grouping means in the analysis of variance. *Biometrics*, 30(3):507–512, 1974. ISSN 0006341X, 15410420. URL <http://www.jstor.org/stable/2529204>.

Shiraishi, T., Miwa, D., Le Duy, V. N., and Takeuchi, I. Selective inference for change point detection by recurrent neural network. *Neural Computation*, 37(1):160–192, 12 2024. ISSN 0899-7667. doi: 10.1162/neco\_a\_01724. URL [https://doi.org/10.1162/neco\\_a\\_01724](https://doi.org/10.1162/neco_a_01724).

Shtekh, G., Kazakova, P., Nikitinsky, N., and Skachkov, N. Applying topic segmentation to document-level information retrieval. In *Proceedings of the 14th Central and Eastern European Software Engineering Conference Russia, CEE-SECR '18*, New York, NY, USA, 2018. Association for Computing Machinery. ISBN 9781450361767. doi: 10.1145/3290621.3290630. URL <https://doi.org/10.1145/3290621.3290630>.

Solbiati, A., Heffernan, K., Damaskinos, G., Poddar, S., Modi, S., and Cali, J. Unsupervised topic segmentation of meetings with bert embeddings, 2021. URL <https://arxiv.org/abs/2106.12978>.

Somasundaran, S. et al. Two-level transformer and auxiliary coherence modeling for improved text segmentation. In *Proceedings of the AAAI Conference on Artificial Intelligence*, volume 34, pp. 7797–7804, 2020.

Song, K., Tan, X., Qin, T., Lu, J., and Liu, T.-Y. Mpnet: masked and permuted pre-training for language understanding. In *Proceedings of the 34th International Conference on Neural Information Processing Systems*, NIPS '20, Red Hook, NY, USA, 2020. Curran Associates Inc. ISBN 9781713829546.

Truong, C., Oudre, L., and Vayatis, N. Selective review of offline change point detection methods. *Signal Processing*, 167:107299, 2020. ISSN 0165-1684. doi: <https://doi.org/10.1016/j.sigpro.2019.107299>. URL <https://www.sciencedirect.com/science/article/pii/S0165168419303494>.

Wang, T. and Samworth, R. J. High dimensional change point estimation via sparse projection. *Journal of the Royal Statistical Society Series B: Statistical Methodology*, 80(1):57–83, 08 2017. ISSN 1369-7412. doi: 10.1111/rssb.12243. URL <https://doi.org/10.1111/rssb.12243>.

Yu, H., Deng, C., Zhang, Q., Liu, J., Chen, Q., and Wang, W. Improving long document topic segmentation models with enhanced coherence modeling. In Bouamor, H., Pino, J., and Bali, K. (eds.), *Proceedings of the 2023 Conference on Empirical Methods in Natural Language Processing*, pp. 5592–5605, Singapore, December 2023. Association for Computational Linguistics. doi: 10.18653/v1/2023.emnlp-main.341. URL <https://aclanthology.org/2023.emnlp-main.341/>.

## A. Proofs

### A.1. Auxiliary Results for Lemma 1

**Proposition A.1** (m-dependent concentration for segment cost). *Fix integers  $1 \leq s \leq e \leq T$  and set  $n = e - s + 1$ . Under Assumptions 4.1–4.2, for every  $x > 0$ ,*

$$\Pr(|\widehat{C}(s, e) - C(s, e)| > x) \leq 4 \exp\left(-\frac{x^2}{8(8m+5)M^2 n}\right).$$

*Proof.* Write

$$\widehat{C}(s, e) - C(s, e) = \underbrace{\sum_{t=s}^e (k(Y_t, Y_t) - \mathbb{E}[k(Y_t, Y_t)])}_{=:A} - \underbrace{\frac{1}{n} \sum_{i=s}^e \sum_{j=s}^e (k(Y_i, Y_j) - \mathbb{E}[k(Y_i, Y_j)])}_{=:B}.$$

Since  $0 \leq k \leq M$ , each centered summand is bounded in absolute value by  $M$ .

We use Janson's inequality for sums with a dependency graph (Thm. 2.1 [Janson \(2004\)](#)). If  $\{X_v\}_{v \in V}$  are centered,  $|X_v| \leq b$ , and  $G = (V, E)$  is a dependency graph with chromatic number  $\chi(G)$ , then for any  $t > 0$ ,

$$\Pr\left(\left|\sum_{v \in V} X_v\right| > t\right) \leq 2 \exp\left(-\frac{t^2}{2\chi(G)|V|b^2}\right). \quad (3)$$

For  $A$ , take  $V_A = \{s, \dots, e\}$  and connect  $t, t'$  when  $|t - t'| \leq m$ . This is a valid dependency graph by  $m$ -dependence (Assumption 4.1): variables further than  $m$  apart are independent. The graph is properly colored by  $t \bmod (m+1)$ , hence  $\chi(G_A) \leq m+1$  and  $|V_A| = n$ . Applying (3) with  $b = M$  and threshold  $t = x/2$  gives

$$\Pr(|A| > x/2) \leq 2 \exp\left(-\frac{x^2}{8(m+1)nM^2}\right). \quad (4)$$

Write  $B = \frac{1}{n}S$  with

$$S := \sum_{i=s}^e \sum_{j=s}^e Z_{ij}, \quad Z_{ij} := k(Y_i, Y_j) - \mathbb{E}[k(Y_i, Y_j)].$$

We consider ordered pairs  $(i, j)$  so that  $|V_B| = n^2$ . Define a dependency graph  $G_B$  on  $V_B = \{(i, j) : s \leq i, j \leq e\}$  by connecting  $(i, j)$  and  $(i', j')$  iff

$$\min\{|i - i'|, |i - j'|, |j - i'|, |j - j'|\} \leq m.$$

Each  $Z_{ij}$  is a function of  $(Y_i, Y_j)$ . If two disjoint vertex sets  $U, W \subseteq V_B$  have no edges between them, then the index sets of  $Y$ 's underlying  $U$  and  $W$  are pairwise more than  $m$  apart in time, hence independent by  $m$ -dependence; therefore  $\{Z_u : u \in U\}$  and  $\{Z_w : w \in W\}$  are independent, as required.

Fix  $(i, j)$ . Let  $T_{ij} := \{k : |k - i| \leq m \text{ or } |k - j| \leq m\}$ ; then  $|T_{ij}| \leq (2m+1) + (2m+1) = 4m+2$ . Any neighbor  $(i', j')$  must satisfy  $i' \in T_{ij}$  or  $j' \in T_{ij}$ . Thus the number of neighbors is at most

$$n|T_{ij}| + n|T_{ij}| \leq 2n(4m+2) = (8m+4)n,$$

so  $\Delta(G_B) \leq (8m+4)n$  and hence  $\chi(G_B) \leq \Delta(G_B) + 1 \leq (8m+4)n + 1 \leq (8m+5)n$  for  $n \geq 1$ . Applying (3) to  $S$  with  $b = M$ ,  $|V_B| = n^2$ ,  $\chi(G_B) \leq (8m+5)n$ , and threshold  $t = nx/2$  yields

$$\Pr(|B| > x/2) = \Pr(|S| > nx/2) \leq 2 \exp\left(-\frac{x^2}{8(8m+5)nM^2}\right). \quad (5)$$

If  $|\widehat{C}(s, e) - C(s, e)| = |A - B| > x$ , then  $|A| > x/2$  or  $|B| > x/2$ . Hence, by (4)–(5),

$$\Pr(|\widehat{C}(s, e) - C(s, e)| > x) \leq 2 \exp\left(-\frac{x^2}{8(m+1)nM^2}\right) + 2 \exp\left(-\frac{x^2}{8(8m+5)nM^2}\right) \leq 4 \exp\left(-\frac{x^2}{8(8m+5)nM^2}\right),$$

where the last inequality uses  $(8m+5) \geq (m+1)$  for all  $m \geq 0$ . This completes the proof.  $\square$

## A.2. Proof of Lemma 4.9

Fix  $[s, e]$  with length  $n = e - s + 1$ . By Proposition A.1, with  $x = \lambda_T \sqrt{n}$ ,

$$\Pr(|\widehat{C}(s, e) - C(s, e)| > x) \leq 4 \exp\left(-\frac{x^2}{8(8m+5)M^2n}\right) = 4 \exp(-4 \log T) = 4T^{-4}.$$

There are  $\frac{T(T+1)}{2}$  segments, so by a union bound,

$$\Pr(\mathcal{E}_T^c) \leq \frac{T(T+1)}{2} \cdot 4T^{-4} = \frac{2(T+1)}{T^3} \leq T^{-1} \quad \text{for all } T \geq 3,$$

since  $T^2 - 2T - 2 \geq 0$  for  $T \geq 3$ . Hence  $\Pr(\mathcal{E}_T) \geq 1 - T^{-1}$ .

## A.3. Proof of Proposition 4.10

Fix a clean segment  $[s, e]$  (i.e.,  $\tau_{k-1} < s \leq e < \tau_k$ ) and  $t \in \{s, \dots, e-1\}$ . Write

$$\Delta\widehat{C}(a, b) := \widehat{C}(a, b) - C(a, b), \quad \Delta_C := C(s, t) + C(t+1, e) - C(s, e).$$

We aim to lower bound

$$[\widehat{C}(s, t) + \widehat{C}(t+1, e) - \widehat{C}(s, e)] + \beta_T = \underbrace{\Delta_C}_{\text{expectation}} + \underbrace{(\Delta\widehat{C}(s, t) + \Delta\widehat{C}(t+1, e) - \Delta\widehat{C}(s, e))}_{\text{deviation}} + \beta_T.$$

On the event  $\mathcal{E}_T$  of Lemma 4.9 (which holds with probability  $\geq 1 - T^{-1}$ ), for all  $1 \leq a \leq b \leq T$ ,

$$|\Delta\widehat{C}(a, b)| \leq \lambda_T \sqrt{b - a + 1}, \quad \lambda_T := 4\sqrt{2}M\sqrt{(8m+5)\log T}.$$

Hence, for any  $s \leq t < e$ ,

$$\begin{aligned} \Delta\widehat{C}(s, t) + \Delta\widehat{C}(t+1, e) - \Delta\widehat{C}(s, e) &\geq -(|\Delta\widehat{C}(s, t)| + |\Delta\widehat{C}(t+1, e)| + |\Delta\widehat{C}(s, e)|) \\ &\geq -\lambda_T(\sqrt{t-s+1} + \sqrt{e-t} + \sqrt{e-s+1}) \\ &\geq -3\lambda_T\sqrt{T}. \end{aligned}$$

Because  $[s, e]$  lies within a single stationary block (Assumption 4.1),  $C(s, e)$  depends only on the length  $n := e - s + 1$ . Denote  $C(n) := C(s, e)$ . Set  $n_1 := t - s + 1$ ,  $n_2 := e - t$ , so  $n = n_1 + n_2$ . For a stationary segment of length  $n$ ,

$$C(n) = (n-1)c_0 - \frac{2}{n} \sum_{l=1}^{n-1} (n-l)c_l, \quad \text{where } c_l := \mathbb{E}[k(Y_1, Y_{1+l})]. \quad (6)$$

Under  $m$ -dependence,  $Y_1$  and  $Y_{1+l}$  are independent for  $l > m$ , hence by bilinearity of the RKHS inner product (no ‘characteristic’ property needed),

$$c_l = \mathbb{E}\langle \phi(Y_1), \phi(Y_{1+l}) \rangle_{\mathcal{H}} = \langle \mathbb{E}\phi(Y_1), \mathbb{E}\phi(Y_{1+l}) \rangle_{\mathcal{H}} = \|\mu_P\|_{\mathcal{H}}^2 =: c_{\infty} \quad (l > m).$$

Define  $\delta_l := c_l - c_{\infty}$ ; then  $\delta_l = 0$  for  $l > m$  and, since  $|k| \leq M$  (Assumption 4.2), we have  $|c_l| \leq M$ ,  $|c_{\infty}| \leq M$ , thus  $|\delta_l| \leq 2M$ . Plugging  $c_l = c_{\infty} + \delta_l$  into (6) and using  $\sum_{l=1}^{n-1} (n-l) = \frac{n(n-1)}{2}$  yields

$$C(n) = (n-1)(c_0 - c_{\infty}) - 2 \sum_{l=1}^{\min(n-1, m)} \left(1 - \frac{l}{n}\right) \delta_l.$$

Let  $V_P := c_0 - c_{\infty}$  and  $S(k) := \sum_{l=1}^{\min(k-1, m)} (1 - l/k) \delta_l$ . Then

$$\Delta_C = C(n_1) + C(n_2) - C(n_1 + n_2) = -V_P - 2(S(n_1) + S(n_2) - S(n)), \quad n = n_1 + n_2.$$

Since  $|\delta_l| \leq 2M$  and  $(1 - l/k) \in [0, 1]$ , we have  $|S(k)| \leq \sum_{l=1}^m |\delta_l| \leq 2mM$  for all  $k \geq 1$ . Also  $|V_P| = |c_0 - c_\infty| \leq 2M$ . Therefore

$$|\Delta_C| \leq |V_P| + 2(|S(n_1)| + |S(n_2)| + |S(n)|) \leq 2M + 2(3 \cdot 2mM) = 2M(1 + 6m) =: C_K.$$

On  $\mathcal{E}_T$ ,

$$[\widehat{C}(s, t) + \widehat{C}(t+1, e) - \widehat{C}(s, e)] + \beta_T \geq -C_K - 3\lambda_T \sqrt{T} + \beta_T.$$

By Assumption 4.5,

$$\beta_T \geq 16M\sqrt{2(8m+5)T \log T} + 2M(1+6m) = 4\lambda_T \sqrt{T} + C_K,$$

so the RHS is at least  $\lambda_T \sqrt{T} > 0$ . Hence

$$\widehat{C}(s, e) < \widehat{C}(s, t) + \widehat{C}(t+1, e) + \beta_T.$$

Since  $\mathcal{E}_T$  holds with probability  $\geq 1 - T^{-1}$  and all bounds above are uniform in  $[s, e]$  and  $t$ , the result holds simultaneously for all clean segments and all splits with that probability.

#### A.4. Proof of Theorem 4.11

Define the empirical penalized criterion

$$L(\boldsymbol{\tau}'_{K'}) := \sum_{k=1}^{K'+1} \widehat{C}(\tau'_{k-1} + 1, \tau'_k) + \beta_T K'$$

and the corresponding population penalized criterion

$$L^*(\boldsymbol{\tau}'_{K'}) := \sum_{k=1}^{K'+1} C(\tau'_{k-1} + 1, \tau'_k) + \beta_T K'.$$

We work on the event  $\mathcal{E}_T$ , which holds with probability at least  $1 - T^{-1}$ .

**Step 1: deviation bound for any fixed segmentation.** Fix an arbitrary segmentation  $\boldsymbol{\tau}'_{K'}$ . For each  $k \in \{1, \dots, K'+1\}$ , let

$$n_k := \tau'_k - \tau'_{k-1} \quad \text{so that} \quad \sum_{k=1}^{K'+1} n_k = T.$$

The segment  $[\tau'_{k-1} + 1, \tau'_k]$  has length  $n_k$ . On  $\mathcal{E}_T$ , the uniform deviation bound gives

$$|\widehat{C}(\tau'_{k-1} + 1, \tau'_k) - C(\tau'_{k-1} + 1, \tau'_k)| \leq \lambda_T \sqrt{n_k} \quad \text{for all } k.$$

Summing this over all segments, we obtain

$$\begin{aligned} \left| \sum_{k=1}^{K'+1} \widehat{C}(\tau'_{k-1} + 1, \tau'_k) - \sum_{k=1}^{K'+1} C(\tau'_{k-1} + 1, \tau'_k) \right| &\leq \sum_{k=1}^{K'+1} |\widehat{C}(\tau'_{k-1} + 1, \tau'_k) - C(\tau'_{k-1} + 1, \tau'_k)| \\ &\leq \lambda_T \sum_{k=1}^{K'+1} \sqrt{n_k}. \end{aligned}$$

By the Cauchy–Schwarz inequality,

$$\sum_{k=1}^{K'+1} \sqrt{n_k} \leq \sqrt{(K'+1) \sum_{k=1}^{K'+1} n_k} = \sqrt{(K'+1)T}.$$

Hence

$$\left| \sum_{k=1}^{K'+1} \widehat{C}(\tau'_{k-1} + 1, \tau'_k) - \sum_{k=1}^{K'+1} C(\tau'_{k-1} + 1, \tau'_k) \right| \leq \lambda_T \sqrt{(K'+1)T}.$$

Since  $K'+1 \leq T$  for any segmentation (there can be at most  $T-1$  change points), we have the simpler bound

$$\left| \sum_{k=1}^{K'+1} \widehat{C}(\tau'_{k-1} + 1, \tau'_k) - \sum_{k=1}^{K'+1} C(\tau'_{k-1} + 1, \tau'_k) \right| \leq \lambda_T T. \quad (7)$$

For the penalized criteria this implies

$$|L(\boldsymbol{\tau}'_{K'}) - L^*(\boldsymbol{\tau}'_{K'})| = \left| \sum_{k=1}^{K'+1} \widehat{C}(\tau'_{k-1} + 1, \tau'_k) - \sum_{k=1}^{K'+1} C(\tau'_{k-1} + 1, \tau'_k) \right| \leq \lambda_T T, \quad (8)$$

since the penalty term  $\beta_T K'$  is identical in both  $L$  and  $L^*$ .

**Step 2: comparison between the empirical minimizer and a competitor.** Let  $\widehat{\boldsymbol{\tau}}_{\widehat{K}}$  be any minimizer of  $L$  over all segmentations. Fix an arbitrary competitor  $\boldsymbol{\tau}'_{K'}$ . We derive a chain of inequalities on  $\mathcal{E}_T$ .

First, apply (8) with  $\boldsymbol{\tau}'_{K'} = \widehat{\boldsymbol{\tau}}_{\widehat{K}}$  to obtain

$$L^*(\widehat{\boldsymbol{\tau}}_{\widehat{K}}) = L(\widehat{\boldsymbol{\tau}}_{\widehat{K}}) - \left[ \sum_{k=1}^{\widehat{K}+1} \widehat{C}(\widehat{\tau}_{k-1} + 1, \widehat{\tau}_k) - \sum_{k=1}^{\widehat{K}+1} C(\widehat{\tau}_{k-1} + 1, \widehat{\tau}_k) \right] \leq L(\widehat{\boldsymbol{\tau}}_{\widehat{K}}) + \lambda_T T. \quad (9)$$

Second, by the optimality of  $\widehat{\boldsymbol{\tau}}_{\widehat{K}}$  for the empirical criterion,

$$L(\widehat{\boldsymbol{\tau}}_{\widehat{K}}) \leq L(\boldsymbol{\tau}'_{K'}). \quad (10)$$

Third, apply (8) with  $\boldsymbol{\tau}'_{K'}$  as given to get

$$L(\boldsymbol{\tau}'_{K'}) = L^*(\boldsymbol{\tau}'_{K'}) + \left[ \sum_{k=1}^{K'+1} \widehat{C}(\tau'_{k-1} + 1, \tau'_k) - \sum_{k=1}^{K'+1} C(\tau'_{k-1} + 1, \tau'_k) \right] \leq L^*(\boldsymbol{\tau}'_{K'}) + \lambda_T T. \quad (11)$$

Combining (9), (10), and (11), we obtain

$$\begin{aligned} L^*(\widehat{\boldsymbol{\tau}}_{\widehat{K}}) &\leq L(\widehat{\boldsymbol{\tau}}_{\widehat{K}}) + \lambda_T T \\ &\leq L(\boldsymbol{\tau}'_{K'}) + \lambda_T T \\ &\leq L^*(\boldsymbol{\tau}'_{K'}) + 2\lambda_T T. \end{aligned}$$

Since this holds for an arbitrary competitor  $\boldsymbol{\tau}'_{K'}$ , we can take the infimum over all segmentations to get

$$L^*(\widehat{\boldsymbol{\tau}}_{\widehat{K}}) \leq \inf_{\boldsymbol{\tau}'_{K'}} L^*(\boldsymbol{\tau}'_{K'}) + 2\lambda_T T.$$

Unwrapping the definition of  $L^*$ , this inequality is exactly (1):

$$\sum_{k=1}^{\widehat{K}+1} C(\widehat{\tau}_{k-1} + 1, \widehat{\tau}_k) + \beta_T \widehat{K} \leq \inf_{\boldsymbol{\tau}'_{K'}} \left\{ \sum_{k=1}^{K'+1} C(\tau'_{k-1} + 1, \tau'_k) + \beta_T K' \right\} + 2\lambda_T T.$$

We have proved that the inequality holds on the event  $\mathcal{E}_T$ , which has probability at least  $1 - T^{-1}$  by Lemma 4.9. This completes the proof.

### A.5. Additional Results for Theorem 4.12

**Lemma A.2** (Signal strength on a mixed segment). *Let  $[s, e]$  contain exactly one true change-point  $\tau_k$  with  $s \leq \tau_k < e$ . Define*

$$n_1 := \tau_k - s + 1, \quad n_2 := e - \tau_k, \quad n := n_1 + n_2, \quad \rho := \frac{n_1 n_2}{n}.$$

Under Assumptions 4.1–4.3,

$$C(s, e) - C(s, \tau_k) - C(\tau_k + 1, e) \geq \rho \Delta_k^2 - \left( (4m+2)M + \frac{(2m^2+2m)M}{n} \right). \quad (12)$$

If, in addition, Assumption 4.4 holds and the segment  $[s, e]$  satisfies  $n_1 \geq \ell_T/2$  and  $n_2 \geq \ell_T/2$ , then

$$C(s, e) - C(s, \tau_k) - C(\tau_k + 1, e) \geq \frac{\Delta_k^2}{4} \ell_T - \left( (4m+2)M + \frac{(2m^2+2m)M}{\ell_T} \right). \quad (13)$$

*Proof.* We prove (12) and then deduce (13).

**Part 1: Proof of (12).** Using  $C(u, v) = \mathbb{E}[\hat{C}(u, v)]$  and expanding the quadratic terms, the diagonal pieces cancel, and we obtain

$$C(s, e) - C(s, \tau_k) - C(\tau_k + 1, e) = \mathbb{E} \left[ \left( \frac{1}{n_1} - \frac{1}{n} \right) \sum_{i,j=s}^{\tau_k} k(Y_i, Y_j) + \left( \frac{1}{n_2} - \frac{1}{n} \right) \sum_{i,j=\tau_k+1}^e k(Y_i, Y_j) - \frac{2}{n} \sum_{i=s}^{\tau_k} \sum_{j=\tau_k+1}^e k(Y_i, Y_j) \right].$$

Write  $\mu_{P_k} := \mathbb{E}[\phi(Y) \mid Y \sim P_k] \in \mathcal{H}$  and recall  $k(x, y) = \langle \phi(x), \phi(y) \rangle_{\mathcal{H}}$ . Introduce the population (independence) proxy by replacing  $\mathbb{E} k(Y_i, Y_j)$  with  $\langle \mu_{\text{dist}(i)}, \mu_{\text{dist}(j)} \rangle_{\mathcal{H}}$ , where  $\text{dist}(i) \in \{k, k+1\}$  indicates the block of  $i$ . This yields the *population term*

$$\frac{n_1 n_2}{n} \left( \|\mu_{P_k}\|_{\mathcal{H}}^2 + \|\mu_{P_{k+1}}\|_{\mathcal{H}}^2 - 2 \langle \mu_{P_k}, \mu_{P_{k+1}} \rangle_{\mathcal{H}} \right) = \rho \|\mu_{P_k} - \mu_{P_{k+1}}\|_{\mathcal{H}}^2 = \rho \Delta_k^2,$$

and a *remainder*  $R$  capturing the  $m$ -dependence corrections.

Let  $\delta_{i,j} := \mathbb{E}[k(Y_i, Y_j)] - \langle \mu_{\text{dist}(i)}, \mu_{\text{dist}(j)} \rangle_{\mathcal{H}}$ . Then  $\delta_{i,j} = 0$  whenever  $|i - j| > m$  by  $m$ -dependence (Assumption 4.1); moreover, by boundedness (Assumption 4.2),  $|\delta_{i,j}| \leq 2M$ . Writing

$$R = \frac{n_2}{nn_1} E_1 + \frac{n_1}{nn_2} E_2 - \frac{2}{n} E_{12},$$

where  $E_1 := \sum_{i,j=s}^{\tau_k} \delta_{i,j}$ ,  $E_2 := \sum_{i,j=\tau_k+1}^e \delta_{i,j}$ , and  $E_{12} := \sum_{i=s}^{\tau_k} \sum_{j=\tau_k+1}^e \delta_{i,j}$ , we bound each piece by counting ordered pairs with  $|i - j| \leq m$ :

$$\begin{aligned} |E_1| &\leq (\text{at most } n_1(2m+1) \text{ pairs}) \cdot 2M = n_1(2m+1) 2M, \\ |E_2| &\leq n_2(2m+1) 2M, \\ |E_{12}| &\leq \left( \sum_{d=1}^m d \right) \cdot 2M = \frac{m(m+1)}{2} \cdot 2M = m(m+1) M, \end{aligned}$$

where the last line counts the cross-boundary pairs with offsets  $d = 1, \dots, m$  once (note the algebra above contributes  $-\frac{2}{n} E_{12}$ , so only left-to-right ordered pairs appear). Consequently,

$$\begin{aligned} |R| &\leq \frac{n_2}{nn_1} n_1(2m+1) 2M + \frac{n_1}{nn_2} n_2(2m+1) 2M + \frac{2}{n} m(m+1) M \\ &= \frac{n_1 + n_2}{n} (4m+2)M + \frac{2m^2 + 2m}{n} M = (4m+2)M + \frac{(2m^2+2m)M}{n}. \end{aligned}$$

Since  $C(s, e) - C(s, \tau_k) - C(\tau_k + 1, e) = \rho \Delta_k^2 + R$ , we obtain (12) from  $R \geq -|R|$ .

**Part 2: Proof of (13).** By Assumption 4.3,  $\Delta_k^2 \geq \Delta_\star^2$ . Under  $n_1, n_2 \geq \ell_T/2$ , the function  $\rho = \frac{n_1 n_2}{n_1 + n_2}$  is minimized at  $n_1 = n_2 = \ell_T/2$ , hence

$$\rho \geq \frac{(\ell_T/2)^2}{\ell_T} = \frac{\ell_T}{4}.$$

Also  $n = n_1 + n_2 \geq \ell_T$ , so

$$-\left((4m+2)M + \frac{(2m^2+2m)M}{n}\right) \geq -\left((4m+2)M + \frac{(2m^2+2m)M}{\ell_T}\right).$$

Combining with (12) yields (13).  $\square$

**Lemma A.3 (Detectability).** *Let Assumptions 4.1–4.8 hold and fix  $\delta > 0$ . Then there exists  $T_\delta$  such that for all  $T \geq T_\delta$  and all intervals  $[s, e]$  containing two consecutive changes  $\tau_k < \tau_{k+1}$ , there exists  $t^* \in [\tau_k, \tau_{k+1} - 1]$*

*and  $t^* - s + 1 \geq \delta_T$ ,  $e - t^* \geq \delta_T$*

*with*

$$C(s, e) - C(s, t^*) - C(t^* + 1, e) \geq \beta_T + 4\lambda_T \sqrt{T} + \delta \beta_T,$$

*where  $\lambda_T := 4\sqrt{2}M\sqrt{(8m+5)\log T}$ .*

*Proof.* Fix  $\delta > 0$ . By Assumption 4.8, for any  $[s, e]$  with  $s \leq \tau_k < \tau_{k+1} \leq e$  there exists  $t^* \in [\tau_k, \tau_{k+1} - 1]$  and  $t^* - s + 1 \geq \delta_T$ ,  $e - t^* \geq \delta_T$  such that

$$C(s, e) - C(s, t^*) - C(t^* + 1, e) \geq c_0 g_k \Delta_\star^2 - C_m. \quad (14)$$

By Assumption 4.4,  $g_k \geq \ell_T$ , hence

$$c_0 g_k \Delta_\star^2 - C_m \geq c_0 \ell_T \Delta_\star^2 - C_m. \quad (15)$$

From Assumption 4.5 there exists  $K_\beta > 0$  and  $T_1$  such that, for all  $T \geq T_1$ ,

$$\beta_T \leq K_\beta \sqrt{T \log T}. \quad (16)$$

Moreover, by the definition of  $\lambda_T$ ,

$$4\lambda_T \sqrt{T} = 16\sqrt{2}M\sqrt{(8m+5)T \log T} =: K_2 \sqrt{T \log T}, \quad (17)$$

with  $K_2 := 16\sqrt{2}M\sqrt{8m+5}$ . Therefore, for all  $T \geq T_1$ ,

$$(1 + \delta)\beta_T + 4\lambda_T \sqrt{T} \leq ((1 + \delta)K_\beta + K_2) \sqrt{T \log T}. \quad (18)$$

Since  $\ell_T/\sqrt{T \log T} \rightarrow \infty$  by Assumption 4.4, there exists  $T_2$  such that, for all  $T \geq T_2$ ,

$$c_0 \ell_T \Delta_\star^2 - C_m \geq ((1 + \delta)K_\beta + K_2) \sqrt{T \log T}. \quad (19)$$

Combining (15), (18), and (19), we obtain that for all  $T \geq T_\delta := \max\{T_0, T_1, T_2, 3\}$ ,

$$c_0 \ell_T \Delta_\star^2 - C_m \geq (1 + \delta)\beta_T + 4\lambda_T \sqrt{T}.$$

Plugging this into (14) for the same  $t^*$  yields

$$C(s, e) - C(s, t^*) - C(t^* + 1, e) \geq (1 + \delta)\beta_T + 4\lambda_T \sqrt{T} = \beta_T + 4\lambda_T \sqrt{T} + \delta \beta_T.$$

All constants are uniform in  $k$  and in  $[s, e]$  because  $\ell_T$ ,  $K_\beta$ , and  $K_2$  do not depend on  $k$ ,  $[s, e]$ .  $\square$

**Lemma A.4 (No overfull estimated segments).** *Let Assumptions 4.1–4.8 hold. Then, with probability at least  $1 - T^{-1}$ , no estimated segment of an optimal penalized partition contains two true changepoints.*

*Proof.* Let  $\widehat{\tau}_{\widehat{K}}$  be any minimizer of

$$L(\boldsymbol{\tau}'_{K'}) = \sum_{r=1}^{K'+1} \widehat{C}(\tau'_{r-1}+1, \tau'_r) + \beta_T K'.$$

Work on the high-probability event

$$\mathcal{E}_T := \left\{ \forall 1 \leq s \leq e \leq T : |\widehat{C}(s, e) - C(s, e)| \leq \lambda_T \sqrt{e - s + 1} \right\},$$

which satisfies  $\Pr(\mathcal{E}_T) \geq 1 - T^{-1}$  by Lemma 4.9.

Suppose, towards a contradiction, that some estimated segment  $[s, e]$  induced by  $\widehat{\tau}_{\widehat{K}}$  contains two consecutive true changepoints  $\tau_k < \tau_{k+1}$  with  $s \leq \tau_k < \tau_{k+1} \leq e$ . Fix any  $\delta > 0$ . By Lemma A.3 there exists  $t^* \in [\tau_k, \tau_{k+1} - 1]$

and  $t^* - s + 1 \geq \delta_T$ ,  $e - t^* \geq \delta_T$  such that

$$G := C(s, e) - C(s, t^*) - C(t^*+1, e) \geq \beta_T + 4\lambda_T \sqrt{T} + \delta \beta_T.$$

On  $\mathcal{E}_T$  we have

$$\begin{aligned} \widehat{G} &:= \widehat{C}(s, e) - \widehat{C}(s, t^*) - \widehat{C}(t^*+1, e) \\ &\geq G - |\widehat{C}(s, e) - C(s, e)| - |\widehat{C}(s, t^*) - C(s, t^*)| - |\widehat{C}(t^*+1, e) - C(t^*+1, e)| \\ &\geq G - \lambda_T (\sqrt{e - s + 1} + \sqrt{t^* - s + 1} + \sqrt{e - t^*}). \end{aligned}$$

Since  $\sqrt{e - s + 1} \leq \sqrt{t^* - s + 1} + \sqrt{e - t^*}$  and each square-root term is at most  $\sqrt{T}$ , we get

$$\widehat{G} \geq G - 2\lambda_T (\sqrt{t^* - s + 1} + \sqrt{e - t^*}) \geq G - 4\lambda_T \sqrt{T}.$$

Hence, by the lower bound on  $G$ ,

$$\widehat{G} \geq \beta_T + \delta \beta_T.$$

If we refine the partition by inserting a split at  $t^*$ , the data-fit part decreases by  $\widehat{G}$  while the penalty increases by  $\beta_T$ , so the net change is

$$\Delta L = -\widehat{G} + \beta_T \leq -(\beta_T + \delta \beta_T) + \beta_T = -\delta \beta_T < 0,$$

contradicting optimality of  $\widehat{\tau}_{\widehat{K}}$ . Therefore, on  $\mathcal{E}_T$ , no estimated segment contains two true changepoints. Since  $\Pr(\mathcal{E}_T) \geq 1 - T^{-1}$ , the claim follows.  $\square$

**Corollary A.5** (No estimated segment contains  $\geq 2$  true changes). *Let Assumptions 4.1–4.8 hold. With probability at least  $1 - T^{-1}$ , every estimated segment of an optimal penalized partition contains at most one true changepoint.*

*Proof.* If an estimated segment contained  $\geq 2$  true changepoints, it would contain some adjacent pair  $(\tau_k, \tau_{k+1})$ . Apply Lemma A.3 within that segment to obtain a split  $t^*$  such that inserting  $t^*$  strictly decreases the penalized cost, exactly as in the proof of Lemma A.4. This contradicts optimality. The high-probability event is the same as in Lemma A.4.  $\square$

**Lemma A.6** (Strict improvement of a mixed segment). *Let Assumptions 4.1–4.3, 4.6 and 4.7 hold. Let  $\mathcal{E}_T$  be the high probability event from Lemma 4.9,*

$$\mathcal{E}_T := \left\{ \forall 1 \leq s \leq e \leq T : |\widehat{C}(s, e) - C(s, e)| \leq \lambda_T \sqrt{e - s + 1} \right\}.$$

Consider an admissible partition  $\boldsymbol{\tau}$  (that is, all its segments have length at least  $\delta_T$ ) and suppose it contains a segment

$$E = [s, e] = [t_L+1, t_R]$$

that contains exactly one true change point  $\tau_k^*$  with  $s \leq \tau_k^* < e$ . Define

$$n_1 := \tau_k^* - s + 1, \quad n_2 := e - \tau_k^*, \quad n := n_1 + n_2.$$

Assume further that

$$n_1 \geq \delta_T \quad \text{and} \quad n_2 \geq \delta_T,$$

so that splitting  $E$  at  $\tau_k^*$  yields two segments that are still admissible. Then, on the event  $\mathcal{E}_T$ , there exists an admissible partition  $\tau'$  (obtained by inserting  $\tau_k^*$  into  $\tau$ ) such that

$$L(\tau') < L(\tau)$$

for all sufficiently large  $T$ .

*Proof.* We work on the event  $\mathcal{E}_T$  throughout.

Let  $\tau$  be an admissible partition that has a mixed segment  $E = [s, e]$  as in the statement, with  $n_1, n_2 \geq \delta_T$ . Define a new partition  $\tau'$  by inserting the true change point  $\tau_k^*$  into  $\tau$  inside the segment  $E$ . That is, we replace the single segment  $[s, e]$  by the two segments  $[s, \tau_k^*]$  and  $[\tau_k^*+1, e]$ , leaving all other segments unchanged. Because

$$n_1 = \tau_k^* - s + 1 \geq \delta_T \quad \text{and} \quad n_2 = e - \tau_k^* \geq \delta_T,$$

every segment in  $\tau'$  still has length at least  $\delta_T$ . Thus  $\tau'$  is admissible under Assumption 4.6. If  $\tau$  has  $K$  change points, then  $\tau'$  has  $K + 1$  change points, so the penalty term in  $L$  increases by  $\beta_T$ .

By definition of  $L$ , the only changes come from the segment  $E$  and the penalty term. Denote

$$\Delta L := L(\tau') - L(\tau).$$

We have

$$\Delta L = \beta_T + \widehat{C}(s, \tau_k^*) + \widehat{C}(\tau_k^*+1, e) - \widehat{C}(s, e).$$

Introduce the population change

$$\Delta C_{\text{pop}} := C(s, \tau_k^*) + C(\tau_k^*+1, e) - C(s, e),$$

and the empirical fluctuation

$$\Delta_{\text{noise}} := (\widehat{C}(s, \tau_k^*) - C(s, \tau_k^*)) + (\widehat{C}(\tau_k^*+1, e) - C(\tau_k^*+1, e)) - (\widehat{C}(s, e) - C(s, e)).$$

Then

$$\Delta L = \beta_T + \Delta C_{\text{pop}} + \Delta_{\text{noise}}.$$

We now control  $\Delta C_{\text{pop}}$  and  $\Delta_{\text{noise}}$ .

The segment  $[s, e]$  contains exactly one true change point  $\tau_k^*$ , so Lemma A.2, inequality (12), applies:

$$C(s, e) - C(s, \tau_k^*) - C(\tau_k^*+1, e) \geq \rho \Delta_k^2 - \left( (4m+2)M + \frac{(2m^2+2m)M}{n} \right),$$

where

$$\rho := \frac{n_1 n_2}{n}, \quad n = e - s + 1, \quad n_1 = \tau_k^* - s + 1, \quad n_2 = e - \tau_k^*.$$

Rewriting, we obtain

$$\Delta C_{\text{pop}} = C(s, \tau_k^*) + C(\tau_k^*+1, e) - C(s, e) \leq -\rho \Delta_k^2 + \left( (4m+2)M + \frac{(2m^2+2m)M}{n} \right).$$

By Assumption 4.3,  $\Delta_k^2 \geq \Delta_*^2$ , so

$$\Delta C_{\text{pop}} \leq -\rho \Delta_*^2 + \left( (4m+2)M + \frac{(2m^2+2m)M}{n} \right).$$

Without loss of generality suppose  $n_1 \leq n_2$ . Then

$$\rho = \frac{n_1 n_2}{n_1 + n_2} = n_1 \cdot \frac{n_2}{n_1 + n_2}.$$

Since  $n_2 \geq n_1$ , we have

$$\frac{n_2}{n_1 + n_2} \geq \frac{1}{2},$$

hence

$$\rho \geq \frac{n_1}{2} = \frac{\min(n_1, n_2)}{2}.$$

Using  $n_1, n_2 \geq \delta_T$ , we obtain

$$\rho \geq \frac{\delta_T}{2}.$$

Consequently,

$$\Delta C_{\text{pop}} \leq -\frac{\delta_T}{2} \Delta_{\star}^2 + \left( (4m+2)M + \frac{(2m^2+2m)M}{n} \right).$$

Since  $E$  is admissible,  $n = e - s + 1 \geq \delta_T$ . Hence

$$(4m+2)M + \frac{(2m^2+2m)M}{n} \leq (4m+2)M + \frac{(2m^2+2m)M}{\delta_T} = \bar{B}_T.$$

We thus obtain

$$\Delta C_{\text{pop}} \leq -\frac{\delta_T}{2} \Delta_{\star}^2 + \bar{B}_T.$$

On the event  $\mathcal{E}_T$ , Lemma 4.9 gives, for any segment  $[u, v]$  of length  $n_{uv} = v - u + 1$ ,

$$|\hat{C}(u, v) - C(u, v)| \leq \lambda_T \sqrt{n_{uv}}.$$

Apply this to the three segments:

$$[s, \tau_k^{\star}] \text{ of length } n_1, \quad [\tau_k^{\star}+1, e] \text{ of length } n_2, \quad [s, e] \text{ of length } n = n_1 + n_2.$$

We obtain

$$\begin{aligned} |\hat{C}(s, \tau_k^{\star}) - C(s, \tau_k^{\star})| &\leq \lambda_T \sqrt{n_1}, \\ |\hat{C}(\tau_k^{\star}+1, e) - C(\tau_k^{\star}+1, e)| &\leq \lambda_T \sqrt{n_2}, \\ |\hat{C}(s, e) - C(s, e)| &\leq \lambda_T \sqrt{n}. \end{aligned}$$

Therefore

$$|\Delta_{\text{noise}}| \leq \lambda_T \sqrt{n_1} + \lambda_T \sqrt{n_2} + \lambda_T \sqrt{n} = \lambda_T (\sqrt{n_1} + \sqrt{n_2} + \sqrt{n}).$$

Using Cauchy–Schwarz,

$$\sqrt{n_1} + \sqrt{n_2} \leq \sqrt{2(n_1 + n_2)} = \sqrt{2n},$$

so

$$\sqrt{n_1} + \sqrt{n_2} + \sqrt{n} \leq \sqrt{2n} + \sqrt{n} \leq (\sqrt{2} + 1)\sqrt{n} < 3\sqrt{n}.$$

Thus

$$|\Delta_{\text{noise}}| \leq 3\lambda_T \sqrt{n} \leq 3\lambda_T \sqrt{T},$$

since  $n \leq T$ .

Combining the previous bounds, we have

$$\Delta L = \beta_T + \Delta C_{\text{pop}} + \Delta_{\text{noise}} \leq \beta_T + \left( -\frac{\delta_T}{2} \Delta_{\star}^2 + \bar{B}_T \right) + |\Delta_{\text{noise}}|.$$

Using the bound on the noise term,

$$\Delta L \leq \beta_T - \frac{\delta_T}{2} \Delta_{\star}^2 + \bar{B}_T + 3\lambda_T \sqrt{T}.$$

By Assumption 4.7, there exists  $T_0$  such that for all  $T \geq T_0$ ,

$$\frac{\delta_T}{2} \Delta_{\star}^2 > \beta_T + \bar{B}_T + 3\lambda_T \sqrt{T}.$$

Fix any  $T \geq T_0$  and define

$$\eta_T := \frac{\delta_T}{2} \Delta_\star^2 - (\beta_T + \bar{B}_T + 3\lambda_T \sqrt{T}) > 0.$$

Then

$$\beta_T - \frac{\delta_T}{2} \Delta_\star^2 + \bar{B}_T + 3\lambda_T \sqrt{T} = -\eta_T < 0,$$

and hence, using the previous bound on  $\Delta L$ ,

$$\Delta L \leq \beta_T - \frac{\delta_T}{2} \Delta_\star^2 + \bar{B}_T + 3\lambda_T \sqrt{T} = -\eta_T < 0.$$

Therefore  $L(\boldsymbol{\tau}') < L(\boldsymbol{\tau})$  for all  $T \geq T_0$  on the event  $\mathcal{E}_T$ . Therefore, for all sufficiently large  $T$  and on  $\mathcal{E}_T$ ,

$$\Delta L \leq -\eta_T < 0.$$

Hence  $L(\boldsymbol{\tau}') < L(\boldsymbol{\tau})$ , which shows that the admissible partition obtained by inserting the true change point  $\tau_k^*$  into the mixed segment  $E$  has strictly smaller penalized cost than  $\boldsymbol{\tau}$ .  $\square$

#### A.6. Proof of Theorem 4.12

Recall the high-probability event  $\mathcal{E}_T$  from Lemma 4.9:

$$\mathcal{E}_T := \left\{ \forall 1 \leq s \leq e \leq T : |\hat{C}(s, e) - C(s, e)| \leq \lambda_T \sqrt{e - s + 1} \right\},$$

where  $\lambda_T = 4\sqrt{2}M\sqrt{(8m+5)\log T}$ , and  $\Pr(\mathcal{E}_T) \geq 1 - T^{-1}$  for all  $T \geq 3$ .

Let  $\mathcal{N}_T$  be the high-probability event from Lemma A.4 (No overfull estimated segments). That lemma states that, under Assumptions 4.1–4.8, for all  $T$  large enough

$$\Pr(\mathcal{N}_T) \geq 1 - T^{-1},$$

and on  $\mathcal{N}_T$ , *no segment of an optimal penalised partition contains two true change points*.

Define

$$\Omega_T := \mathcal{E}_T \cap \mathcal{N}_T.$$

Then  $\Pr(\Omega_T) \geq 1 - 2T^{-1} \rightarrow 1$  as  $T \rightarrow \infty$ . We will show that on  $\Omega_T$  and for  $T$  large enough,

$$\forall 1 \leq k \leq K : \min_{0 \leq j \leq \hat{K}} |\hat{\tau}_j - \tau_k^*| \leq \delta_T. \quad (20)$$

This will imply (2), because  $\Pr(\Omega_T) \rightarrow 1$ .

So fix  $T$  large and suppose  $\Omega_T$  holds. Let  $\hat{\tau}_{\hat{K}} \in \mathcal{P}_T(\delta_T)$  denote the optimal penalized partition (the Embed-KCPD estimator).

We now argue by contradiction. Suppose that there exists at least one true change point that is not localized within  $\delta_T$ . That is, assume there exists

$$k^* \in \{1, \dots, K\} \quad \text{such that} \quad \min_{0 \leq j \leq \hat{K}} |\hat{\tau}_j - \tau_{k^*}^*| > \delta_T.$$

Fix such an index  $k^*$ .

Let  $E$  be the segment of the estimated partition  $\hat{\tau}_{\hat{K}}$  that contains  $\tau_{k^*}^*$ . Concretely, there exists  $r \in \{1, \dots, \hat{K}+1\}$  such that

$$E = [s, e] = [\hat{\tau}_{r-1} + 1, \hat{\tau}_r],$$

with the convention  $\hat{\tau}_0 = 0$ ,  $\hat{\tau}_{\hat{K}+1} = T$ , and

$$\hat{\tau}_{r-1} < \tau_{k^*}^* \leq \hat{\tau}_r.$$

By Lemma A.4, on  $\mathcal{N}_T$  no optimal penalized segment contains two true change points. Since  $E$  contains  $\tau_{k^*}^*$ , it must therefore contain *exactly one* true change point, namely  $\tau_{k^*}^*$ . Thus  $E$  is a *mixed* segment with exactly one true change.

Next, because  $\tau_{k^*}^*$  is at distance strictly greater than  $\delta_T$  from every estimated change point, we have

$$\begin{aligned}\tau_{k^*}^* - \hat{\tau}_{r-1} &> \delta_T, \\ \hat{\tau}_r - \tau_{k^*}^* &> \delta_T.\end{aligned}$$

In terms of subsegment lengths inside  $E$ , define

$$n_1 := \tau_{k^*}^* - s + 1 = \tau_{k^*}^* - \hat{\tau}_{r-1}, \quad n_2 := e - \tau_{k^*}^* = \hat{\tau}_r - \tau_{k^*}^*.$$

Then

$$n_1 \geq \delta_T + 1 > \delta_T, \quad n_2 \geq \delta_T + 1 > \delta_T. \quad (21)$$

Since  $\delta_T \rightarrow \infty$ , for  $T$  large enough we can simply write  $n_1 \geq \delta_T$  and  $n_2 \geq \delta_T$ .

Note also that  $E$  itself is admissible by construction, since  $\hat{\tau}_{\hat{K}} \in \mathcal{P}_T(\delta_T)$  implies that  $e - s + 1 = \hat{\tau}_r - \hat{\tau}_{r-1} \geq \delta_T$ .

Because  $E$  contains exactly one true change point  $\tau_{k^*}^*$  and  $n_1, n_2 \geq \delta_T$ , and both  $E$  and the partition are admissible, we are exactly in the setting of Lemma A.6 (Strict improvement of a mixed segment, admissible split). More precisely, Lemma A.6 applies to:

- the partition  $\tau := \hat{\tau}_{\hat{K}}$ , which belongs to  $\mathcal{P}_T(\delta_T)$  by Assumption 4.6; - the segment  $E = [s, e]$ , which is an element of that partition and contains exactly one true change  $\tau_{k^*}^*$ ; - the subsegment lengths  $n_1, n_2$  which satisfy  $n_1 \geq \delta_T$  and  $n_2 \geq \delta_T$ .

Lemma A.6 states: on the event  $\mathcal{E}_T$  and under Assumptions 4.1–4.3, 4.6 and 4.7, for all sufficiently large  $T$ , there exists a new admissible partition  $\tau'$  obtained from  $\tau$  by *inserting* the true change point  $\tau_{k^*}^*$  into the segment  $E$  such that

$$L(\tau') < L(\tau).$$

In particular, since we are on  $\Omega_T \subseteq \mathcal{E}_T$ , and  $T$  is large, when we take  $\tau = \hat{\tau}_{\hat{K}}$ , Lemma A.6 yields an admissible partition  $\tau'$  with

$$L(\tau') < L(\hat{\tau}_{\hat{K}}).$$

But this contradicts the definition of  $\hat{\tau}_{\hat{K}}$  as an optimal minimizer of  $L(\cdot)$  over  $\mathcal{P}_T(\delta_T)$ .

Therefore, our assumption that there exists  $k^*$  with

$$\min_{0 \leq j \leq \hat{K}} |\hat{\tau}_j - \tau_{k^*}^*| > \delta_T$$

must be false on  $\Omega_T$  for all sufficiently large  $T$ .

Equivalently, on  $\Omega_T$  and for all large  $T$ ,

$$\forall 1 \leq k \leq K : \min_{0 \leq j \leq \hat{K}} |\hat{\tau}_j - \tau_k^*| \leq \delta_T.$$

Since  $\Pr(\Omega_T) \rightarrow 1$  as  $T \rightarrow \infty$ , we obtain (2).

Finally, the  $O_p(\delta_T)$  bound on the maximal localization error follows directly from (2): for any  $\varepsilon > 0$  there exists  $T_0$  such that for all  $T \geq T_0$ ,

$$\Pr\left(\max_{1 \leq k \leq K} \min_{0 \leq j \leq \hat{K}} |\hat{\tau}_j - \tau_k^*| \leq \delta_T\right) \geq 1 - \varepsilon,$$

which is exactly  $\max_k \min_j |\hat{\tau}_j - \tau_k^*| = O_p(\delta_T)$ .

This completes the proof.

## B. Computational complexity of KCPD

The computational complexity of kernel change point detection (KCPD) combined with the PELT algorithm is well understood (Arlot et al., 2019). Let  $n$  denote the number of observations and  $c$  the cost of evaluating the kernel function. In the exact kernel setting, forming the  $n \times n$  Gram matrix requires  $O(n^2 c)$  time and  $O(n^2)$  memory. Given the Gram matrix,

segment costs can be evaluated in  $O(1)$  time via cumulative sums, and PELT achieves linear expected time under its standard pruning assumptions (Killick et al., 2012) (with a quadratic worst case). Consequently, in the exact-kernel setting the overall time and memory are typically dominated by Gram-matrix precomputation, i.e.,  $O(n^2c)$  time and  $O(n^2)$  memory.

We use cosine similarity implemented as a dot product on unit-normalized embeddings (i.e., a linear kernel on normalized features). For the standard KCPD within-segment scatter cost

$$C(s, e) = \sum_{t=s}^e k(t, t) - \frac{1}{e-s+1} \sum_{t=s}^e \sum_{u=s}^e k(t, u),$$

the linear kernel yields the closed form

$$C(s, e) = L - \frac{1}{L} \left\| \sum_{t=s}^e y_t \right\|_2^2, \quad L = e - s + 1,$$

since  $k(t, u) = y_t^\top y_u$  and  $\|y_t\|_2 = 1$ . Precomputing prefix sums  $P_t = \sum_{i=1}^t y_i$  allows evaluating  $C(s, e)$  in  $O(d)$  time using  $P_e - P_{s-1}$ , where  $d$  is the embedding dimension, without forming the Gram matrix. This reduces memory to  $O(nd)$  (or  $O(d)$  if embeddings are streamed and only prefix sums are stored), and makes the PELT optimization close to linear in  $n$  in practice, in addition to the one-pass embedding computation.

## C. Additional Experimental Results

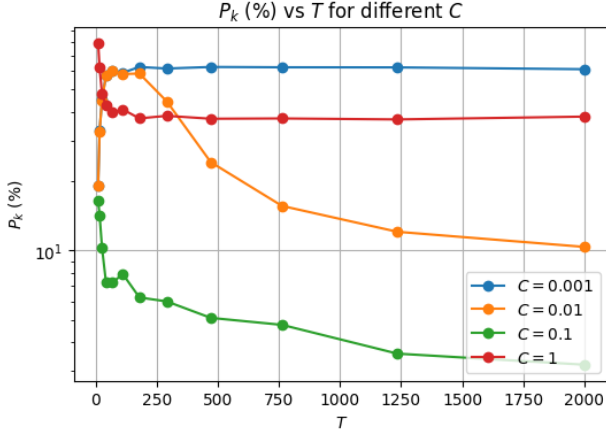


Figure 3.  $P_k$  error (%) versus sequence length  $T$  for Embed-KCPD applied to synthetically generated short-range dependent text data with GPT-4.1,  $m = 20$ , for multiple values of  $C$  and sBERT embeddings.

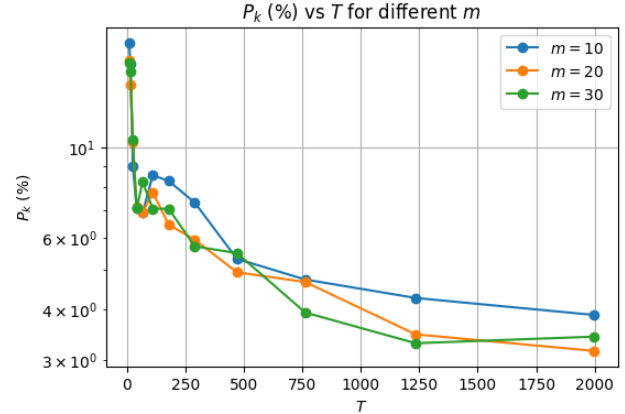


Figure 4.  $P_k$  error (%) versus sequence length  $T$  for Embed-KCPD applied to synthetically generated short-range dependent text data with GPT-4.1,  $C = 0.1$ , for multiple values of  $m$  (number of sentences in LLM generation) and sBERT embeddings.

Figures 3 and 4 indicate the effect of varying  $C$  and  $m$  on  $P_k$ .

## D. Experimental Details

### D.1. Statistics of Dataset

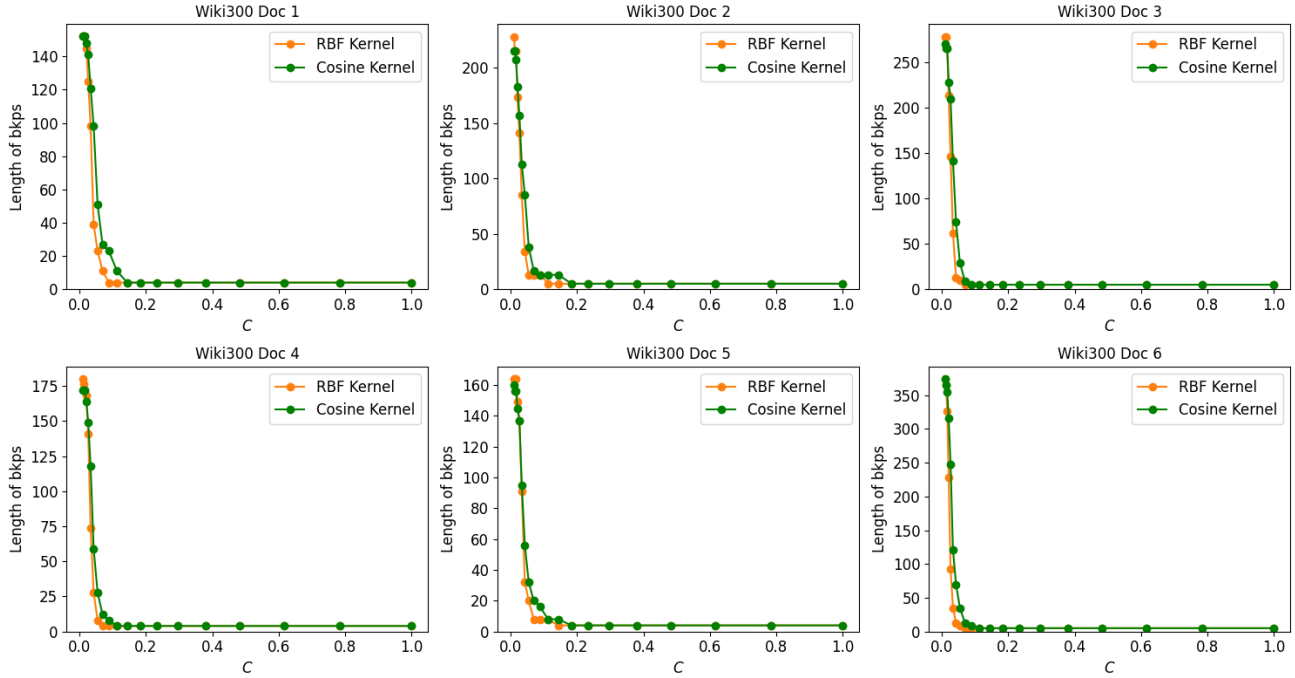
Here is the summary of all datasets we used in the experiments. Table 3 present the summary statistics for each dataset: total number of documents, number of segments per document, number of sentences per segment.

### D.2. Implementation details

Embed-KCPD is implemented with the ruptures library (Truong et al., 2020), using its kernel-based change-point implementation. We use ruptures' median heuristic to set the bandwidth for the RBF Kernel.

Table 3. Statistics of Datasets in Our Experiments.

Dataset	Documents	Segments per Document	Sentences per Segment
Choi (3-5)	100	10	4.0
Choi (6-8)	100	10	7.0
Choi (9-11)	100	10	9.9
Choi (3-11)	400	10	7.0
Wiki-300	300	7.6	26.0
Wiki-50	50	8.2	7.5
Elements	118	7.7	2.9
arXiv	20	9.5	7.1


 Figure 5. Sensitivity of the number of detected segments to the hyperparameter  $C$  on Wiki-300.

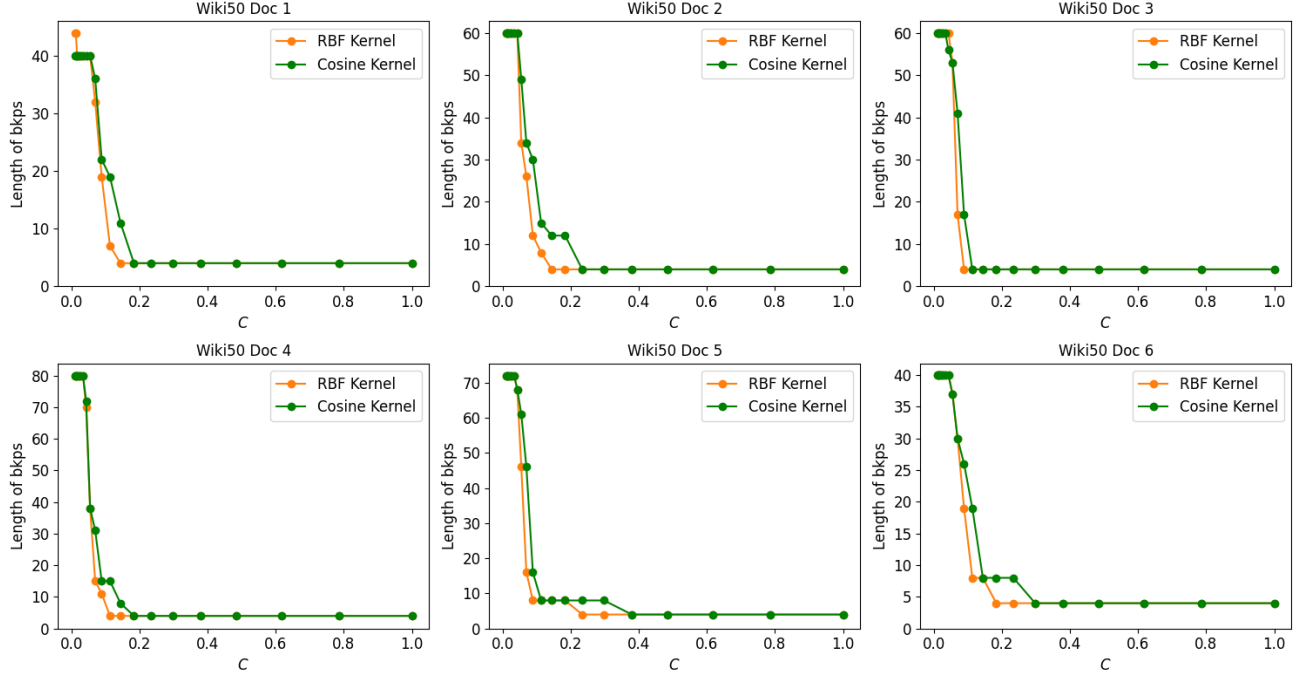
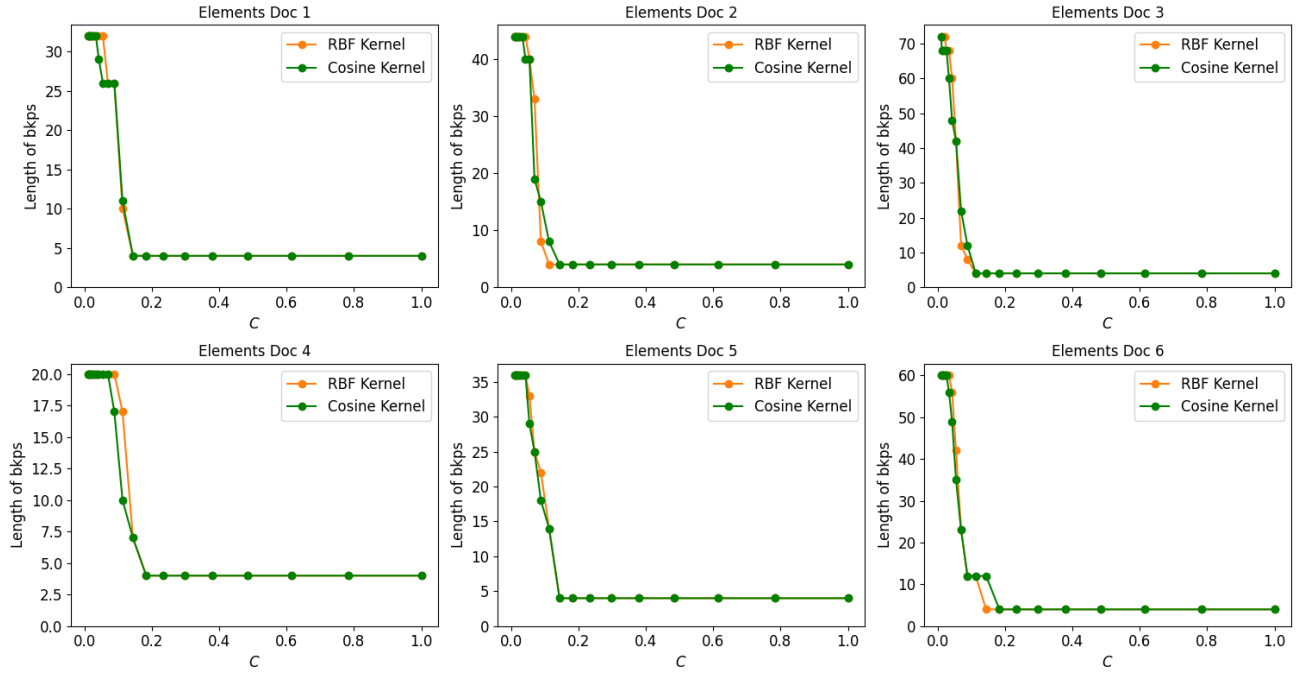
We compute text-embedding-3-small sentence representations using the OpenAI API. For the LLM-based experiment, we use GPT-4.1 via the same API; the total API cost for running all experiments is below \$20. All other embedding backbones are computed locally with the sentence-transformers library using the corresponding pretrained models.

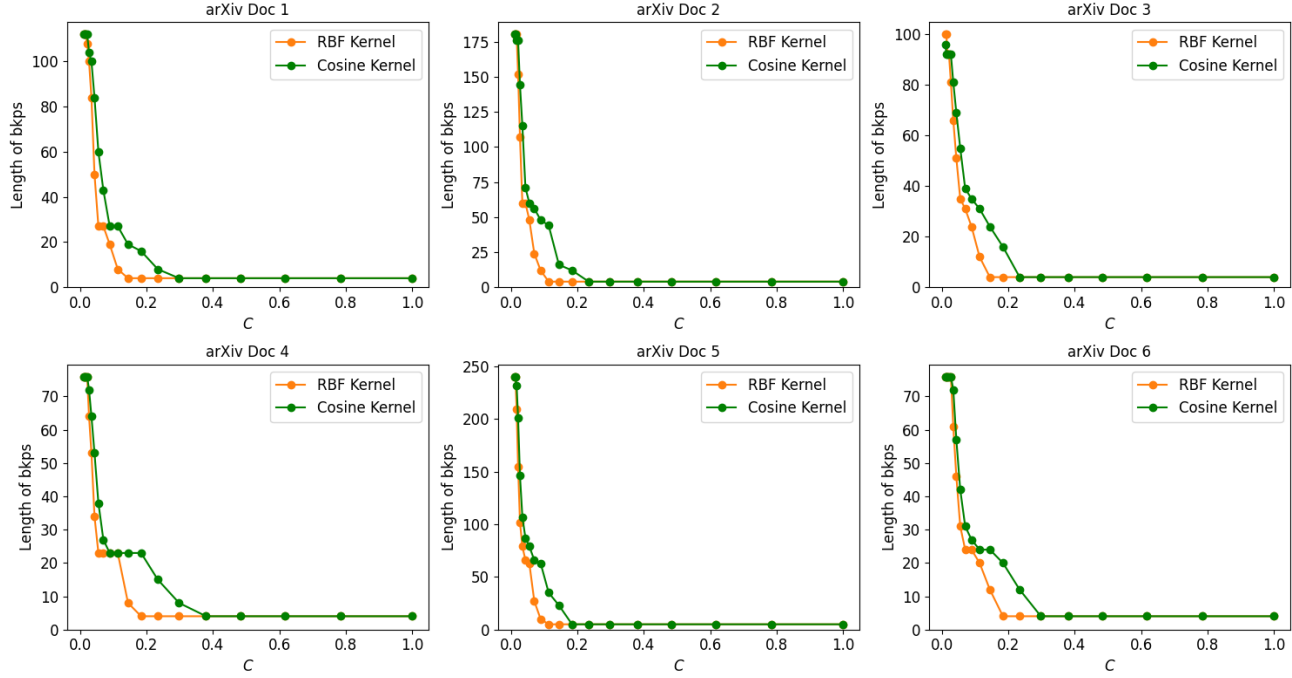
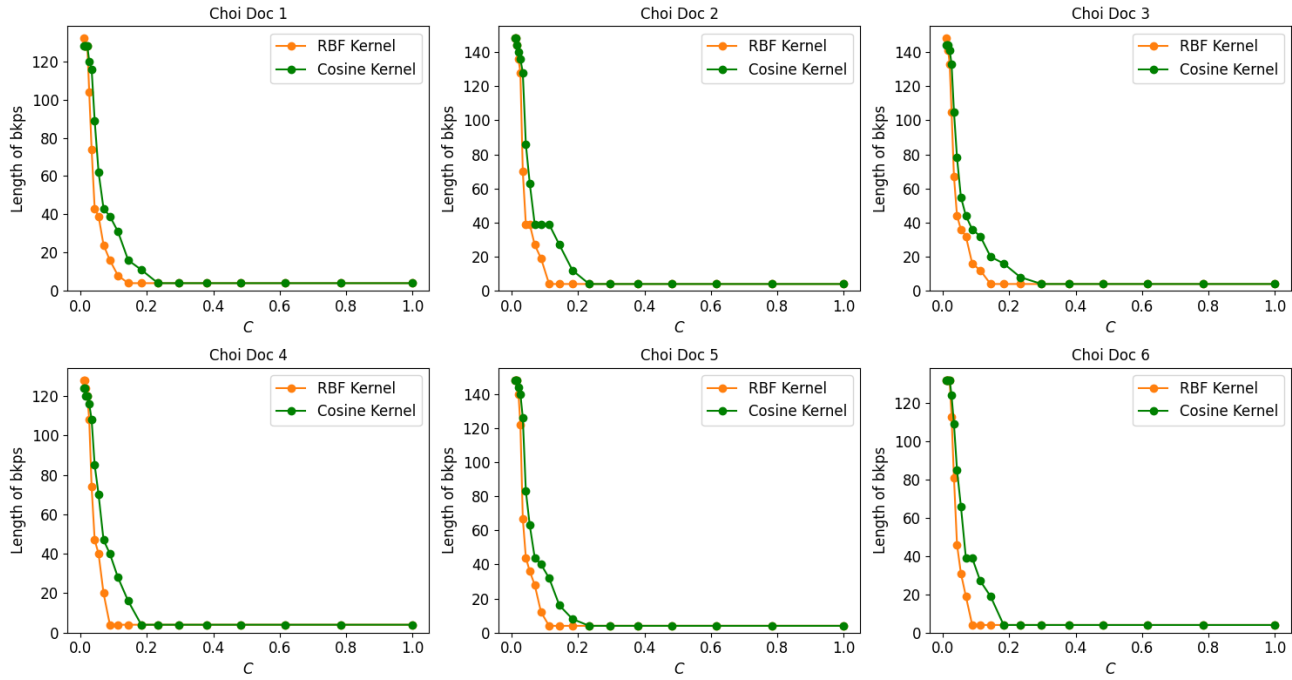
For all baseline methods, we use the fine tuned hyperparameters from the original papers or from widely used public implementations.

All code and implementation is available as supplementary materials.

### D.3. Optimal $C$ via Elbow Method

For each dataset, we randomly sample 6 documents and, for each document, run Embed-KCPD over a small logarithmically spaced  $C$  in the range  $[10^{-2}, 10^0]$ . The elbow point of the curve relating the number of detected change points to  $C$  is selected per document, and the final  $C$  is set to the average of these six values (see Fig. 5 for 6 documents from Wiki-300 datasets). Across datasets, the resulting elbow locations are highly consistent (see Figures 6-9). We therefore fix  $C = 0.06$  for the RBF kernel and  $C = 0.088$  for the cosine kernel across all experiments to ensure a fair, unsupervised comparison. Since  $\beta_T = C\sqrt{T \log T}$ , the effective penalty adapts to sequence length.


 Figure 6. Sensitivity of the number of detected segments to the hyperparameter  $C$  on Wiki-50.

 Figure 7. Sensitivity of the number of detected segments to the hyperparameter  $C$  on Elements.


 Figure 8. Sensitivity of the number of detected segments to the hyperparameter  $C$  on arXiv.

 Figure 9. Sensitivity of the number of detected segments to the hyperparameter  $C$  on Choi (3-11).

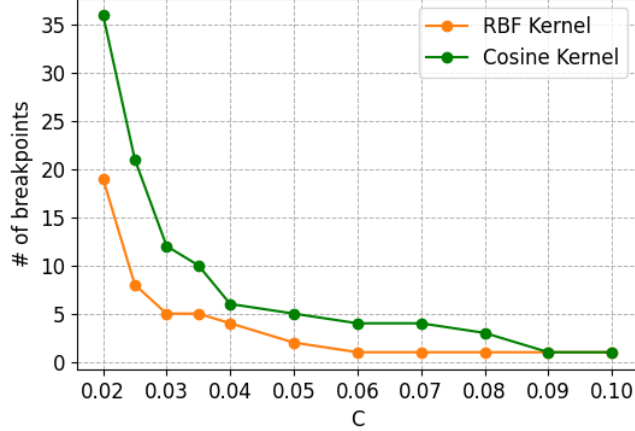


Figure 10. Sensitivity of the number of detected segments to the hyperparameter  $C$  on Taylor Swift’s tweet stream.

#### D.4. Sensitivity of $C$ on $P_k$ and WD

To validate the robustness of our method with respect to  $C$  around the identified sweet spots,  $C = 0.088$  for the kCPD kernel and  $C = 0.06$  for RBF kernel, we conduct a sensitivity analysis on arXiv and Elements datasets. As shown in Figure 11, we vary  $C$  within the range  $[0.08, 0.10]$  for kCPD and  $[0.05, 0.07]$  for RBF. Across these intervals, both the  $P_k$  and WD metrics remain stable, indicating that performance is not sensitive to small perturbations of  $C$  near the optimal region.

#### D.5. $m$ -dependent Data Generation

Sentences are generated sequentially using GPT-4.1 with the fixed prompt: *Give me one more sentence to naturally continue the text specific on [Topic]. Do not add any preamble just answer with one sentence. [Input Sentences]*.

For a target sequence length  $T$ , the number of change points,  $K = \lceil 2 \log T \rceil$ , increases slowly with  $T$ . Candidate change-point locations are sampled uniformly without replacement from  $1, \dots, T$ , and converted into  $K + 1$  segment lengths via successive differences. No explicit minimum segment length constraint is imposed. Instead, segment lengths are controlled implicitly: as  $T$  grows, the average segment length  $T/(K + 1)$  also grows, ensuring that segments become longer asymptotically, consistent with the minimum spacing requirement in Assumption 4.4.

#### D.6. arXiv Dataset Generation

We construct new dataset based on the recent paper abstracts for text segmentation. The generation process is as follows:

- Select the first 1000 papers from arXiv published after August 2025.
- Randomly sample 20 values between 5 and 20 to determine the number of unique abstracts per document.
- For each document, randomly select the corresponding number of abstracts, shuffle them to concatenate into a single text. Repeat this process 20 times to obtain 20 documents.

Full list of 1000 arXiv papers used to built this dataset part of the supplementary materials.

#### E. Data Disclaimer

We collected tweets from Taylor Swift’s official Twitter/X account (@taylorswift13) between January 2020 and May 2025, totaling approximately 400 posts. These tweets are public user-generated content, and our study only uses them for aggregate statistical analysis. In compliance with Twitter/X’s Terms of Service, we do not redistribute the dataset; instead, our paper reports only derived analyses. Code to extract these tweets using X API part of the supplementary materials.

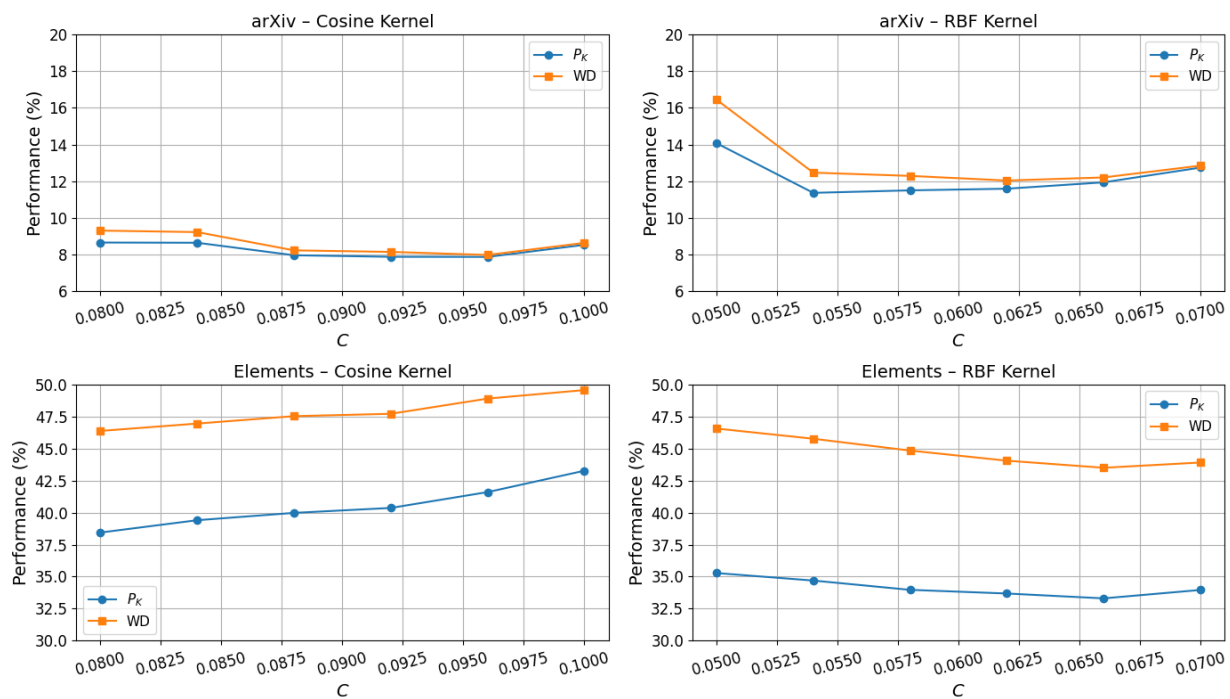


Figure 11. Sensitive of  $C$  with cosine and RBF kernel on Elements and arXiv dataset.